The Effects of Gravels on Piping

Bachelor Thesis Assignment Civil Engineering

Arjen Zagema

Assignment period: April 2020 – July 2020

Beesel, Limburg

10-06-2020

Bachelor thesis Civil Engineering at Witteveen+Bos

The effects of gravels on piping

Student:
Name: A.G. Zagema
Student number: S1950517
E-mail address: a.g.zagema@student.utwente.nl

Internal supervisor:
Name: dr. ir. T.M. Duong
E-mail address: t.m.duong@utwente.nl

External supervisor:
Name: ir. G.P. van Rinsum
E-mail address: guido.van.rinsum@witteveenbos.com

Educational program:
Study: BSc Civil Engineering
Institute: University of Twente
Department: Water Management
Period: Third year, Module 12

Preface

This thesis completes the bachelor Civil Engineering at the University of Twente. The research has been carried out under supervision and in collaboration with Witteveen+Bos.

Although the plan was to do research at the office of Witteveen+Bos in Utrecht, the Corona-crisis had decided differently. I have completed this thesis research completely from my student room in Enschede. Despite this obstruction, I have been able to work well with my supervisors by Skype and e-mail.

I would like to thank Witteveen+Bos. In particular, I would like to thank ir. Guido van Rinsum for his help, advice, and recommendations on the subject in question during this thesis. The support with D-Geo Flow software from Msc Martijn. Asschert was appreciated, thanks for that. Also, I want to the thank group leader ir. Joost Lansink for his help and advice in the early stages of this thesis. Finally, I would also like to thank my supervisor from the university dr. ir. T.M. Duong for her help and advice.

Arjen Zagema
Enschede, July 2020

Summary

Dikes ensure that the Netherlands is protected against flooding like in the year 1953. In that year, the high water level and waves overpowered the floods defences. To prevent such disasters, dikes are regularly assed for certain failure mechanisms, including 'piping'. The Sellmeijer method is often used during the piping assessment in the dikes. But, this method has some complications when the surface contains gravels. In the southern part of the Netherlands, like Limburg, is a gravel surface located underneath the dike. Therefore, further investigation about the piping with gravel surface is needed to properly assess the dikes in Limburg. The goal of this thesis research is to gain more insight into the piping mechanism for a gravel layer. To achieve this research objective, the main research question will be answered; (i) what is the effect of a gravel layer on the piping mechanism?; (ii) this question has been divided into the four sub-questions: What are the hydro-geological effects of a gravel layer in the subsurface?; (iii) what factors influence the piping mechanism? What is the effect of the thickness of the gravel layer on the piping mechanism? ; (iv) what is the effect of the permeability of the gravel layer on the piping mechanism?

Deltares has developed the modelling program D-Geo Flow, which can evaluate situations to analyse piping for several dike situations on piping. This program is a groundwater flow model connected with a particle transport model, which is based on the method of Sellmeijer. This program has been used to answer these questions. The results showed that the thickness and the permeability has a significant effect on piping when the gravel layer is located below a small sand layer. The critical head difference decreases when the permeability or the thickness of the gravel layer increases. Furthermore, the critical pipe-length is not at the middle of the seepage length as the Wettelijk instrumentarium voor de Beoordeling (WBI) suggests, but varies in different situations. The main conclusions of this thesis research is that the gravel layer in the subsurface has an significant effect on the piping mechanism since a gravel layer in the subsurface will lead to the decreasing of the critical head difference, depending on their thickness and permeability. For further research is recommended to validate the results with field observation.

Table of Content

1 Introduction

1.1 Context

'Hoogwaterbeschermingsprogramma' is one of the current flood protection programs in the Netherlands, which is an alliance of the water boards and the Rijkswaterstaat. They are working together to strengthen the dikes for the water-safe Netherlands in 2050. Besides that, all dikes must be assessed according to the Wettelijk instrumentarium voor de Beoordeling (WBI) before 2023. This assessment focuses on several failure mechanisms of the dikes, including piping. The dikes located along the river Meuse in Limburg are also assessed in this program. In this area, these dikes are mainly located on the gravel containing subsurface. For the assessment of those dikes is more insight into the effects of gravel on the piping mechanism required since the current procedure is unsuitable for these situations. Therefore, this research study intends to gain more insight into the piping mechanism in situations with a gravel layer in the subsurface.

1.2 Problem description

Dikes are constructed to protect the delta areas from the impact of high-water levels. Dikes are designed to offer sufficient resistance to various failure mechanisms, such as macro stability failure, overtopping, failure of revetments, and piping. In most cases, these dikes consist of impervious clay material and are constructed on a sand or gravel layer. With the failure mechanism 'piping', water flows through a sand or gravel layer under the dike. If this water flows with a high velocity, this current can cause the subsurface to wash out on the polder side. This erosion can ultimately cause so-called 'pipes' developing under the dike, which can ultimately lead to the failure of the dike.

In the current consultancy practice, the Sellmeijer method is used during the dike assessment. But there are some issues with this method regarding the gravels. In some parts of the Netherlands (Limburg), there is a gravel surface located underneath the dike. Therefore, further investigation about the piping with gravel surface is needed to properly assess the dikes in Limburg.

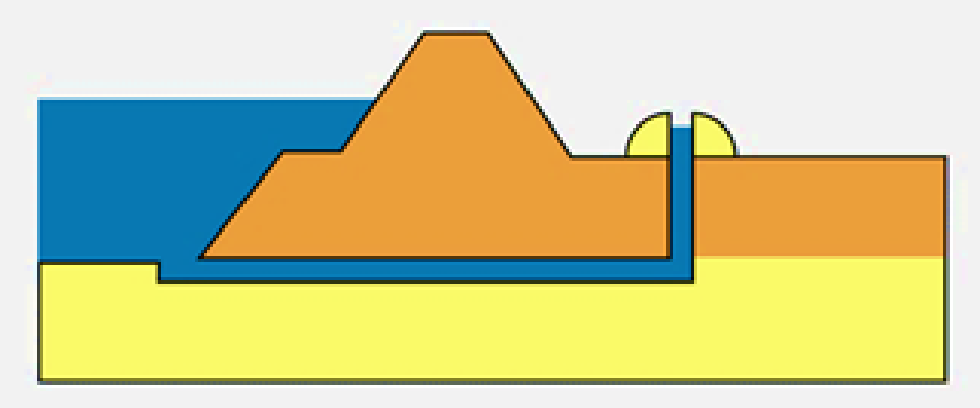

Figure 1. Simplification of piping.

1.3 Research relevance

In recent years, many research studies have been focussing on piping. Nevertheless, there are large unknowns in the piping mechanism in a gravel layer. Also, the recent observations of the gravel surfaces in Limburg make this research study very relevant for the geotechnical engineering field.

1.4 Research objective and questions

This Bachelor's thesis is to investigate the effect of a gravel layer with piping. The research objective of this study is:

"to gain more insight into the piping mechanism for a gravel layer. '

The research objective will be achieved by answering the following main research question:

"What are the effects of a gravel layer on the piping mechanism?"

The main research question is divided into the sub-questions below:

Question 1: What are the hydrogeological effects of a gravel layer in the subsurface?
Question 2: What factors influence the piping mechanism?
Question 3: What are the effects of the thickness of the gravel layer on the piping mechanism?
Question 4: What are the effects of the permeability of the gravel layer on the piping mechanism?

1.5 Thesis outline

This thesis will answer the stated research question and sub-questions. In Chapter 2, the hydrogeologic effects of a gravel layer are addressed. Furthermore, Chapter 2 describes the influencing factors related to gravels on the piping mechanism. Chapter 3 explains the methodology to answer research questions 3 and 4. Chapter 3 elaborates also on the verification of the D-Geo Flow. Chapter 4 gives the answers to questions 3 and 4 by presenting the results of the D-Geo Flow simulations. Chapter 5 discusses the results and findings. In the end, Chapter 6 and 7 draw the conclusions from this thesis and provide recommendations for further research. The report refers sporadically to the Appendices, which are located at the end part of this thesis report.

2 Background

This chapter contains the answers to the first 2 sub-question 1 and 2, thus the hydrological effects of a gravel layer will be described and the effects on piping will be discussed. Furthermore, the piping mechanism is the subject of this thesis, therefore it is necessary to describe this failure mechanism, to better understand this thesis.

2.1 Geological properties

Gravel is a loose aggregation of unconsolidated rock fragments. Table 1 shows the classification of the (Standardization, 2002) for the identification of soil shown. This international standard has three sub-categories for gravel, namely, fine, medium, and coarse. Natural gravel depositions are a geological feature because of weathering and erosion of rocks. The gravel is mainly transported by rivers. Therefore, the gravel is rounded due to the abrasion during the transport. In this sediment transport process, rivers pile up the gravel in large quantities. (Tikkanen, 2020)

Table 1. Particle size fractions according to the ISO 14688 (Standardization, 2002)

Soil group	Particle size fractions	Size range (in mm)
Fine soil	Clay	<0.002
	Silt	0.002 - 0.063
Coarse soil	Fine sand	0.063 - 0.20
	Medium sand	0.20 - 0.63
	Coarse sand	0.63 - 2.0

	Fine gravel	2.0 – 6.3
	Medium gravel	6.3 – 20
	Coarse gravel	20 – 63
Very coarse soil	Cobble	63 – 200
	Boulder	200 – 630
	Large boulder	>630

2.2 Hydrogeological properties

It is required to understand the hydrogeological effects of the gravel layer in the subsurface because the piping mechanism depends not only on geological properties but also on the hydrogeology in the dike area. The distribution and movement of groundwater in the soil are called hydrogeology. This includes three main mechanisms in the subsurface:

(1) The water gets into the ground;
(2) The water flow in the subsurface;
(3) The interaction of groundwater with the surrounding soil.

Among 3, mechanisms (2) and (3) are relevant for this study since they are present in the piping mechanism. The two main drivers in the piping mechanism are the groundwater flow velocity in the subsurface and the transport of particles. The geological properties of the gravel and gravel layers need to be studied before going into depth about the groundwater flow and the dynamics behind the transport of particles.

The movement and storage of the fluid in the sediment is mainly influenced by two factors: the permeability and porosity of the soil. The ability of the soil to allow water or soil air to pass through is indicated by the permeability coefficient (k) and the porosity is the fraction of the volume pores or voids over the total volume of the soil. Both properties are depending on the pore spaces presented in the soil and how much they relate to each other (Fryar & Mukherjee, 2019). Gravel has a very high permeability which is mainly induced by the particle sizes of the soil. There is always a grain size distribution that contains more than one-grain size. This grain size distribution also influences the number of voids in the soil. The relatively large particles allow space in the soil since the particles are not small enough to fill the voids. Therefore, the soil has more voids and the fluid has more space to pass, which eventually increases the permeability of the soil (Koopmans & Janssen, 2018).
The groundwater flow velocity depends mainly on the particle size hence it increases rapidly when the particle size is increased, and the particle surface rugosity because the velocity decreases significantly with increased surface roughness (Mulqueen, 2005). The groundwater flow is very much related to the permeability.
In reality, often gravel layers are present with compositions of sand and organic matter. This results in a more spread grain size distribution, this grain variation in the soil increases the strength of the soil (Wiersma & Hijma, 2018) which can drastically reduce the permeability of the soil (Mulqueen, 2005). The reason for this is that sand in the pores of the gravel layer determines mainly the permeability of the layer (Koopmans & Janssen, 2018). Because the sand in the pores will block the passage of water through the soil, which is affecting the flow of the water, thus the permeability decreases when sand is present in the pores of the gravel layer.
This is one of the reasons for the large variance in permeability measurements in the areas close to the Meuse in Limburg. The measured permeability of the gravel layers was between 85 and 184 m/day (Koopmans & Janssen, 2018) whereas the permeability of clean fine gravel is around 864 m/day (Texas Geosciences, 2020). The main reason for this remarkable difference is that the gravel layers are not connected. This slows the groundwater flow by the sand and organic materials since they have a large impact on the permeability (Koopmans & Janssen, 2018).

It is also possible in the natural environment that not the entire layer is made of gravels but only the gravels nests are present in the layer. These nests of gravel are causing a higher groundwater rise height depending on their position below the dike because the permeability of these nests is higher than the surrounding soil (Koopmans & Janssen, 2018).

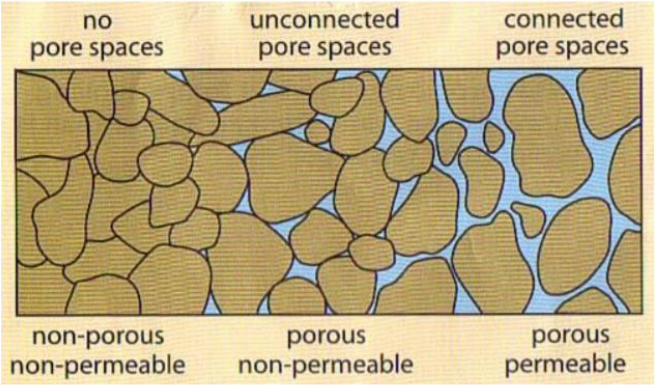

Figure 2. Variation in pore spaces. (UC Denver, 2020)

Aquiclude, aquitard, and aquifer are the 3 main different types of underground layers. Aquicludes are solid impermeable layers with extremely low permeability. Aquitards are layers with low permeability which restrict the groundwater flow from one aquifer to another. Water bearing layers are aquifers, these layers consist of soil with high permeability where groundwater flow is possible. Therefore, gravel is acting as a very good aquifer even better as sand layers. (Fryar & Mukherjee, 2019)

Figure 3 shows a schematization of the subsurface layers and the dike above. In this situation, the dike is made of impermeable clay and is very cohesive therefore restricts the groundwater flow in the dike with an aquifer located below the dike. The aquifer is made of gravel.

This thesis study focusses on the effect of the aquifer on the critical gradient and not on the effect of the layers above the pipe. Although, it is worth mentioning that the cohesive layer and dike considerably affects on the initiation and progression of piping when the aquifer is made of sandy gravel. The thickness of these overlying clay influences the mechanism because, with a thicker overlying clay layer(s), the critical gradient is larger. (Wang, Chen, He, & He, 2016) The critical gradient initiates the development of the entire pipe. Also, the pipe develops more rapidly since the erosion rate is higher. And, the average flow velocity in the pipe is larger caused by the low deformability of the thicker clay layer.

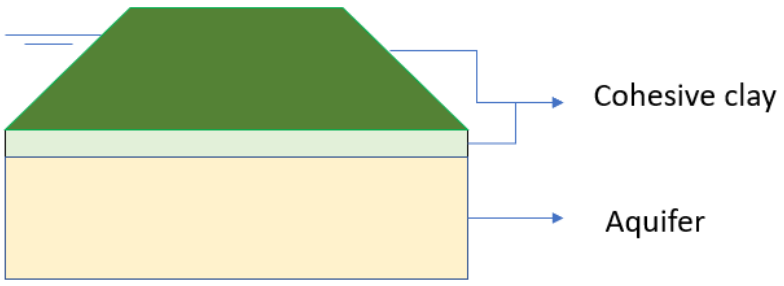

Figure 3. The schematization of the dike situation. This figure is not at scale.

2.3 Piping process

The main function of a dike is to defend the mainland from the water. This flood defence function is possible lost due to the piping failure mechanism. Piping is a phenomenon that can occur at high water levels of the open water in situations where the water level difference is large. The decline is the difference in height between the water level of open water and the inland groundwater level. The actual word 'open water' refers to rivers, canals, lakes, or seas. The groundwater flow, caused by the water level difference, can lead to backward erosion and eventually the forming of shallow channels in the sand below the dike. These channels can evolve, and, in the end, open water relates to the inland water level. (Vrijling, 2010) This result of this process can be seen in Figure 1, where the channel is fully developed and has reached the open water. The backward erosion ultimately results in a reduction of the ground stability with serious consequences for the safety of the area behind the flood defence. Piping will described more in detail in the following sections.
Important to note, the process is described for a sand subsurface, since the process for gravel is unknown, at this moment. For most dikes in the Netherlands, the dike intersection looks like the situation in Figure 4. The dike is made from cohesive clay or peat, which is acting as a relatively confined aquifer (Hart, 2018). The inland surface is also covered with clay or peat layers. The dike is on top of sand layer, which is a relatively unconfined aquifer. In this example, the open water is represented by a river and the inland open water is a ditch with water level equal to the groundwater level. In this first situation, Figure 4, the water level is equal to both sides of the dike, so no water pressure difference is present between the open water and inland water.

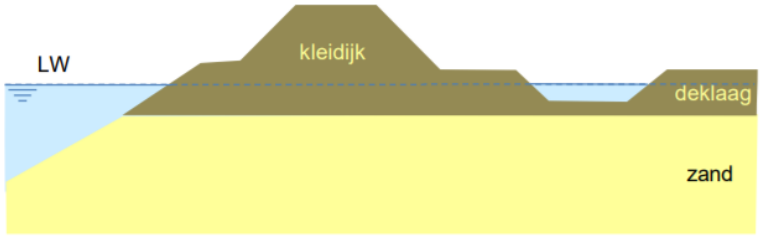

Figure 4. Situation without water level difference between the open water and the inland water. (Hart, 2018)

The water level in the open water can rise, for example during a period of heavy rainfall. An increase in the water levels has the effect of increasing the water pressures in the sand layer, as a result of the start of horizontal groundwater flow in the sand layer (Vrijling, 2010). This means that there is water overpressure in the sand layer relative to the inland surface layer. The intensity of this horizontal groundwater flow depends, among other things, on the incision of the river in the sand layer. Often there is one covering layer, the so-called foreland, present on the outside of the dike. During the high-water level period, there is a water overpressure in the sand layer relative to the surface layer. When the water pressure in the sand aquifer then exceeds the weight of the clay or peat layer, the groundwater in the sand layer will force a way up through the cohesive surface layer (Hart, 2018). This layer will tear and burst. Then, wells arise at the surface layer. When the water produces enough upward force, the water flows from the sand layer to the well since this is the way of the least resistance. The sand is torn up due to the water pressure difference and pushed upwards by the water rising upwards, which is also shown in Figure 5. The sand will be dropped around the well, where a sand crater is formed.

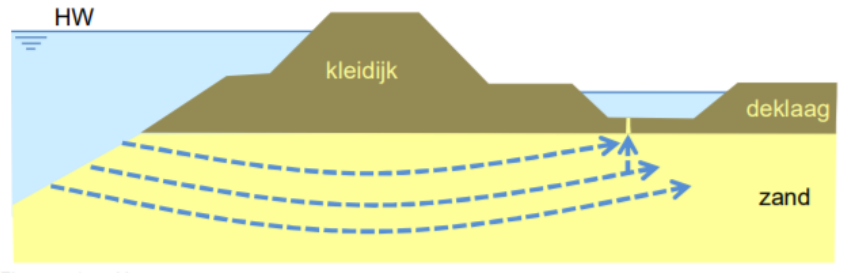

Figure 5. A well is created by the heaving. (Hart, 2018)

In Figure 6, a hollow space is created in the sand layer at the location of the eruption channel, which later expands towards the river. This is called backward erosion. (Vrijling, 2010) The well is starting to become more visible. The channel is located at the top side of the sand layer, close underneath the clay layer. There are two possibilities at this point:

1. This erosion process tends to stop by itself because of the increased resistance in the pipe. As the channel grows toward the open water, the flow rate decreases until the critical gradient of the dike. In this case, the well has only produced clear water without sand. The critical head difference is the maximum water-level difference whereby the forces acting on the grains in the pipe are still in equilibrium (Hart, 2018). This critical gradient will play an important role in the assessment of the piping mechanism since 'failure' does not mean the same for every method. When the channel continues to grow and exceeds the critical gradient of the pipe, the channel will eventually grow to the point of the entrance which is the side of the open water. When the length of the pipe increases, the average gradient of the sand layer (which is still left) does also increases.
2. When this average gradient has passed the critical gradient, the pipe cannot stop growing and will reach the point of the entrance at the open water. The erosion process does not stop and the well is carrying sand to the surface of the land, like in Figure 6. For this situation, the vertical groundwater flow due to the water pressure difference in the clay layer is so big that the effective pressure in the subsurface is reduced to zero. In this scenario, the grains are pushed to the well resulting in a pipe underneath the impervious clay layer (the dike).

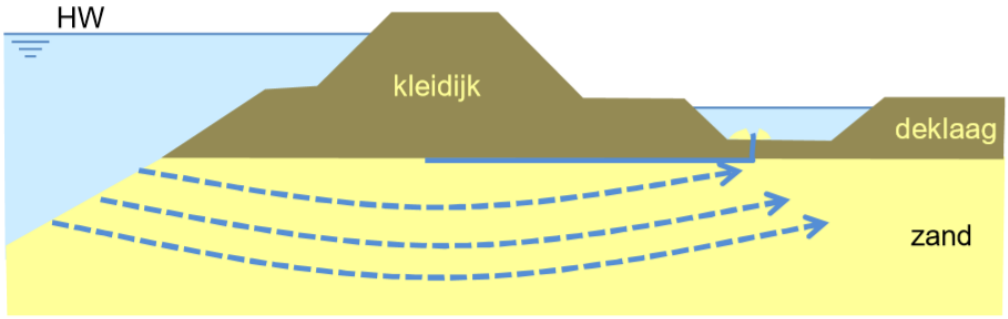

Figure 6. The pipe has reached the critical gradient. (Hart, 2018)

When the channel has arrived at the entrance point, the channel is growing back and is clearing out the sand. So, the channel becomes bigger and reaches the land again. In Figure 7, the channel is fully developed, in this situation, the entrance of the channel is located on the left side of the dike. However, when the decay over the dike is large enough, an open connection will be reached between the entry point and the outdoor water. In that case, the current, produced by the pipe and with it the erosion increases progressively, the dike can sag and eventually collapse.

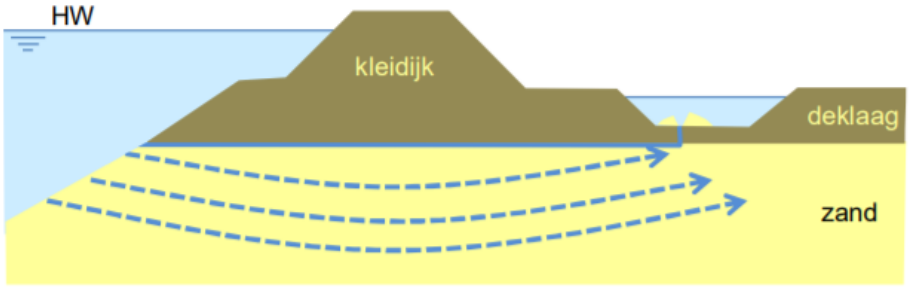

Figure 7. The channel has reached open water. (Hart, 2018)

2.4 The transport of particles

The interaction of the groundwater with the surrounding soil is the large driver in the piping mechanism. In this study case, the surrounding soil is the gravel layer, therefore the interaction with the gravel layer will be discussed. A single gravel particle has more weight than a single sand particle because the volume of gravel is larger and they have relatively the same density therefore larger forces from the groundwater flow are required to exceed the critical forces to transport the grain. The critical gradient is the hydraulic gradient for which the effective vertical stresses become zero, in other words, the pore pressure exceeds the vertical effective stress. This 'critical' pore pressure is caused by the water level differences between the sides of the dike, this difference is generating a pressure gradient over the vulnerable grains directly below the cohesive clay layer. The transport of particles is depending on the equilibrium of the particle where the two main forces are the weight due to the acting gravitational forces and the drag induced by the groundwater flow. (Vrijling, 2010) The particle starts to motion when this equilibrium is failed thus pore pressure crosses the vertical effective stress. In Figure 8 is the transport of particles showed on the micro-level.

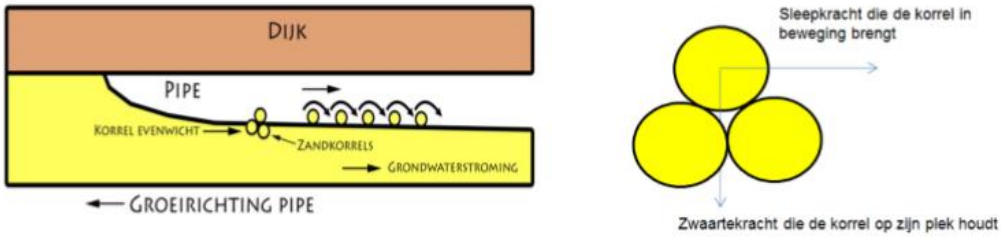

Figure 8. The transport of particles on the micro-level. (Vrijling, 2010)

As already mentioned, in the natural environment are gravel layers mixed with sand particles. These sand and gravel particles do not interact the same with the groundwater. Several experiments on piping with sandy gravels are executed in recent years. These experiments have shown that, as expected, the sand content starts to wash out first before the gravel particles start to motion (Skempton, 1994). On the one hand, the permeability of the gravel layer is larger than the permeability of the sand layer, which allows more water to pass the soil and increases the flow velocity in the soil. And, on the other hand, the resistance of a gravel particle is larger than the resistance of the sand particle whereby more drag is needed to transport the particle.
Because the sand particles need less drag to motion since there resistance is lower. But there are several remarkable results of these experiments.
A significant amount of sand content is washed out by the piping mechanism at a hydraulic gradient which is far lower than the critical gradient determined by the theory of (Terzaghi, 1925). The piping of the sand content

starts at a hydraulic gradient which is 1/3 -1/5 of the determined critical gradient of the entire sample. Even more remarkable is that these hydraulic gradients are far less than the critical gradient for a sample which is made completely out of the sand component. The reason for this difference between the values of the experiment and theory is that a large part of the load is carried on the gravel particles resulting in small pressure on the sand grains (Skempton, 1994).

So, sand grains are more vulnerable to piping in gravel environments than in sand environments. This yields only for internally unstable sandy gravels. The stability of the material is determined with the filter rule of (Terzaghi, 1925) which is shown below. In the equation, the material is separated into two parts: the fine (D15) and coarse components (d85). When the material satisfies this equation, the material is stable.

$$f = \frac{D'_{15}}{d_{85}} < 4 \qquad \text{Equation 1}$$

The piping for the sand content in internally stable sandy gravels starts at approximately the critical gradient determined by the theory of (Terzaghi, 1925). The results from the analyse of the sandy gravels along the Meuse river in Limburg have concluded that the gravel layer is internally unstable (Koopmans & Janssen, 2018). Therefore, sand grains start to wash out in an early stage in this area. It is unknown when the gravel particles start to wash out. The experiments of (Skempton, 1994) have concluded at the critical gradient of the sample, there was no movement remarked of the gravel particles and stayed stable although the pipe covered the whole area. During the test, the flow switches from laminar to turbulent flow at the point the Reynolds number exceeds a value of 5. The Reynolds number is a dimensionless measure designed to predict the behaviour of the flow of fluid. The flow close to the fine particles is laminar, but the flow is turbulent when the flow is surrounded by coarser grains (Van Beek, 2018) This transition area is located at a grain size of approximately 0.4 mm (Hoffmans & Van Rijn, 2017).

2.5 Influencing factors of the gravel layer on piping

Piping is a complex groundwater flow mechanism influenced by several factors. This section elaborates on the relevant factors regarding the piping mechanism. Two of these factors will be used to investigate the effect of a gravel layer on the piping mechanism, which is the main research question of this thesis. Before that, it is required to know which factors can be used to investigate the effect. Figure 9 is a schematization of the dike area.

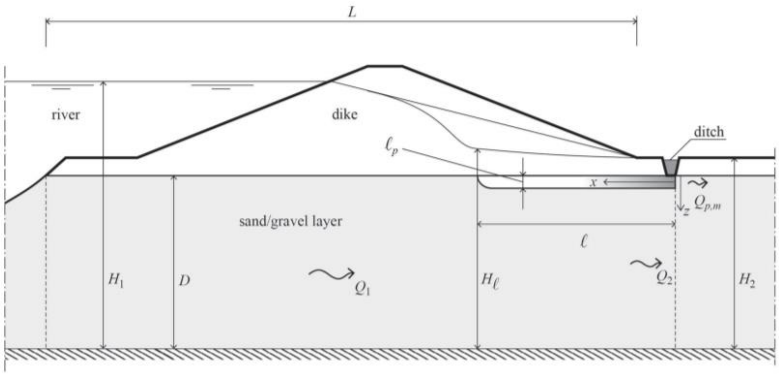

Figure 9. Schematization of the dike situation. This figure is not at scale. (Hoffmans & Van Rijn, 2017)

- The thickness of the aquifer appears to be an important parameter for the critical gradient (Van Beek, 2015). In Figure 9 is the thickness indicated by *D.* When the depth of the aquifer increases, the area of flow increases and, more water will flow towards the exit point of the pipe (Robbins & Van Beek, 2015). Resulting in higher flow velocities close to the pipe and a smaller critical gradient.

- A larger permeability allows a larger volume of water to pass the soil, as mentioned earlier in the thesis. The permeability influences the critical gradient (Van Beek, 2015). It is difficult to say what exactly the effect is of the permeability on the critical gradient, due to the large dependency of a large number of influencing factors on the permeability, such as the grain size, relative density, uniformity and the anisotropy of the soil.
- The distance between the entry on the riverside and exit point on the polder-side is the so-called seepage length. Furthermore, this is the length of the pipe when it is fully developed. The gradient caused by the water level difference, (H1-H2), between those two points is acting over this seepage length. In Figure 9 is the seepage length is represented by *L*. The larger the seepage length, the less pressure is acting on the grains, because the gradient is spread over a longer distance, so over 'more grains (Van Beek, 2015). So, the larger the seepage length, the larger the critical gradient.
- The anisotropy of the soil has an effect on the critical head difference (Stoop, 2018) When a soil has different properties in different axes, then the soil is anisotropy, which is the opposite of isotropy. In other words, the water flows differently vertically then horizontally, see also Figure 10. Anisotropy (Kh>Kv) increases the critical head difference. This can be explained since less water flows in the vertical direction so less water flow towards the pipe, which eventually lowers the pressure surrounding the pipe and the exit (Stoop, 2018).

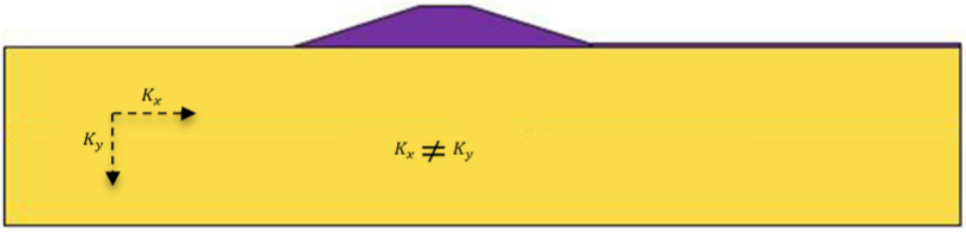

Figure 10. Clarification of anisotropy. (Stoop, 2018)

- The grain size influences the erosion process. The sand grains are located directly below the cohesive clay layer and are vulnerable to pipe development. The water level differences can cause the critical forces for the development of the pipes by lift, drag, and frictional forces. The larger the grain size, the more of these forces is required from the groundwater flow to transport these particles. Although, this factor has a relatively minor effect on the piping mechanism (Van Beek, 2015). In large-scale experiments is a slightly negative trend visible in the results, which means that the critical gradient decrease when the grain size increases.

The effect of the gravel layer on the piping mechanism will be investigated by doing a sensitivity analysis with two factors. This methodology and results of these analysis will be explained in Chapter 3 and 4. The following factors are chosen to analyse their effect on the piping mechanism:

1. The permeability of the aquifer.
2. The thickness of the aquifer.

3 Methodology

This Chapter describes the methodology to answer the last two sub-research questions. From Chapter 2 can be concluded that the permeability of gravel layer can be significantly larger than the sand layer and the thickness is an influencing factor on the piping mechanism. The main research question is to give the effect of the gravel layer on the piping mechanism. In this thesis, the effect is divided into two parts: the effect of the permeability on piping and the thickness on piping. These factors are selected since they seem interesting to investigate in Chapter 2. The effect of the permeability and the thickness will be studied with the support of D-Geo Flow. This is a modelling program which is very suitable for piping analysis. An extensive explanation of the program can be found in Appendix A.

To answer the research questions, the approach is divided into two parts.

1. First, the input data is discussed together with the geometry of the verification model and then verified using the calculation rules of (Sellmeijer, 2011). This verification model is needed to check whether the model responds correctly to the input parameters. The method of Sellmeijer is explained in Chapter 3.1.3.
2. In this second step, the research questions will be answered. The schematization model will be made which will be adjusted during the experiments. Two experiments will be performed, where will be focussed on determining the effect of the permeability and the thickness. The schematization is like the starting point of the experiment. The schematization model is based on the verification model to ensure that the results of the analysis are reliable within this thesis. The verification model contains only one homogenous aquifer, but during the experiments is an aquifer containing two layers needed therefore the verification model does not suit the experiments. Finally, the effect of the thickness and the permeability of the second layer in the subsurface are calculated by the D-Geo Flow model and compared with an adjusted method of Sellmeijer, which will be explained later on.

3.1Verifying the D-Geo Flow model with Sellmeijer method

The verified model is partly based on the findings of (M. van Rees, 2019) and (N. Stoop, 2018), who both used D-GeoFlow during their research projects. The model will be calculated with several varieties of parameters and compared with the calculation rules of (Sellmeijer, 2011) to verify the model and the behaviour of the model. The water level of the river will be increased with 0.02 meters each time step over 7 days. The reason for this decision is to increase the accuracy of the results and to prevent numerical instability. The grid function implements a grid in the dike and the aquifer, which is needed for the groundwater flow model. The grid is designed by the input parameters, the coarseness of the mesh, and a pipe. The coarseness of the mesh is equal to 2.5 meters and the grid-elements along the pipe will be 6 times smaller than the coarseness of the mesh. These values are assumed since they are also used in the D-GeoFlow manual of Deltares. The grid function affects the output and run time of the model. The model will be described and explained in the following sections.

3.1.1 The geometry

The model consists of a levee, aquifer, and blanket. In Figure 12, the dimensions of the basic model are shown. The geometry of the verification model is based on the profile generator of HKV. This generator selected three levee geometries from the file Actueel Hoogtebestand Nederland (AHN). This database consists out of all dike areas in the Netherlands, where the only used filter was piping sensitive areas. The three geometries and the mean geometry are shown in Figure 11. The mean geometry will be used for the verification model.

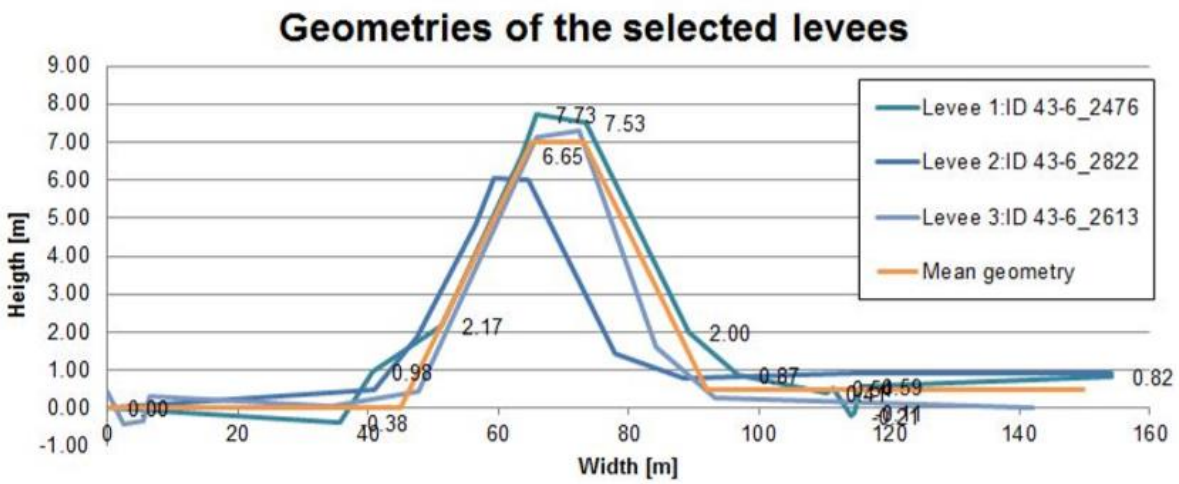

Figure 11. Generated geometries of the selected levees. (Van Rees, 2019)

There is chosen to implement an aquifer with a thickness of 30 meters, to be sure that the critical head will be exceeded during the simulations. D-Geo Flow gives the output of the critical head difference only when the water level has reached the critical head difference, with a thickness of 30 meters is almost guaranteed that the model will give the critical head difference. Figure 12 shows the geometry of the verification model.

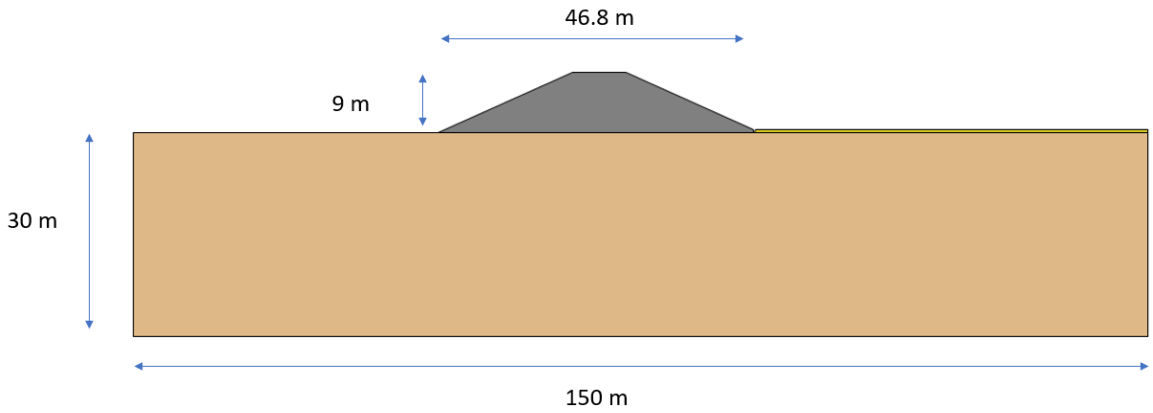

Figure 12. The geometry verification model.

The relevant properties of the elements are provided in Table 2. The aquifer has multiply permeabilities and d70 since these will be used during the verification. The properties of the levee and the blanket are similar to the values used in the D-GeoFlow manual of Deltares and the study of (Van Rees, 2019). There are two parameters constant for all materials, which is the white's constant (η=0.25) and the bedding angle of 37 degrees. These values are calibrated for the Sellmeijer method by experiments (Van Beek & Hoffmans, 2017). The model is set in stationary mode and independent from time which means that the compressibility of the material and water is zero.

Table 2. Material properties.

Element	Hydraulic conductivity [m/d]	D70 [µm]
Levee	0.01	200
Blanket	0.002	200
Aquifer	5	200
	10	200
	2	200
	3	300
	5	100
	10	200
	20	150

3.1.2 Boundary conditions

The boundary conditions are assigned to represent the reality, the effects of the outside world are described in those boundaries. The model is using four different types of boundaries and is depicted in Figure 13. For simplification reasons are the lines AG and GF assigned with the no-flow boundary, which means that these boundaries do not influence the model. The boundaries AG and EF are located at the distance of three times the depth of the aquifer because then these boundaries have only a small influence on the potential distribution of the model (Frank et al., 1987). The seepage boundary is assigned to the lines BC and DE, although almost no seepage of water will be measured at these locations since these boundaries are located below impermeable materials. The line AB is located at the riverside of the dike and does represent the high-water level flow, which can initiate the piping mechanism. This period is showed in Figure 14. The line CD represents a ditch and is also the exit point of the model. This head boundary has a constant head value of h=0. This type of exit point is required since the heave condition is rejected for D-GeoFlow. The line EF is also assigned to a constant head of h=0 because there is assumed that the water body is at rest, therefore there is hydrostatic pressure.

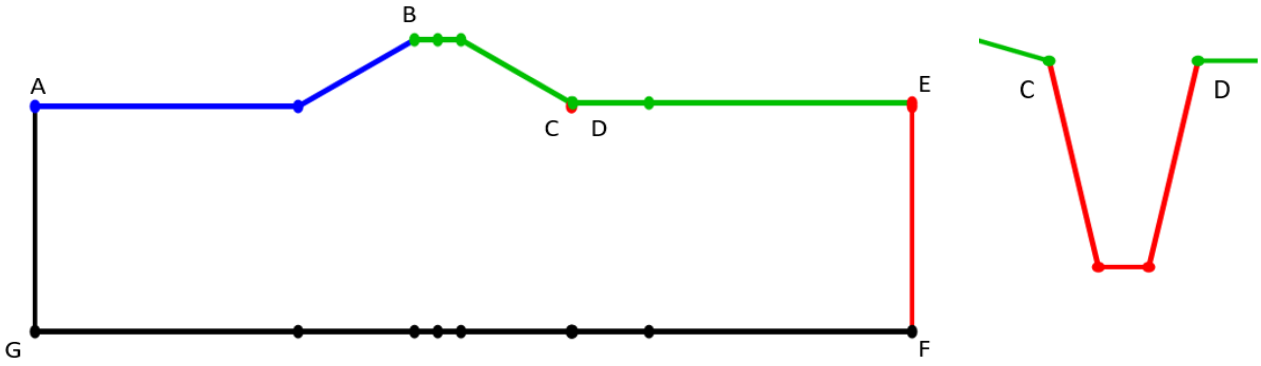

Figure 13. The boundary conditions in D-GeoFlow.

The overview of the assigned boundaries is shown in Table 3. The model is performed in stationary mode, which means that there is no storage of water, so the groundwater flow is independent of time. The high-water curve of the river is given in Figure 14. The high-water level curve of the river is linear because the model is independent of time. So, the critical gradient is calculated for each water level of the river without considering the previous water levels.

Table 3. The boundary conditions.

Line	Boundary condition
AB	Specified head boundary
BC	Seepage boundary
CD	Constant head boundary
DE	No flow boundary
EF	Constant head boundary
FG	No flow boundary
AG	No flow boundary

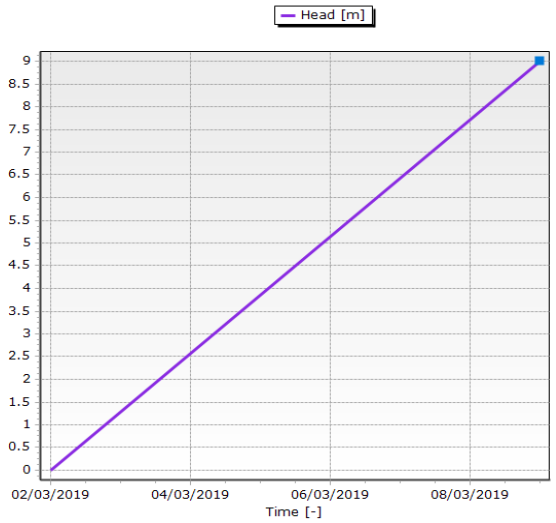

Figure 14. The high-water level curve of the river.

3.1.3 Verification

The answers to research question 3 and 4 are relying on the D-Geo Flow model. To gain confidence in the D-Geo Flow model results, a basic D-Geo Flow model is designed with the same setting and configuration as (Sellmeijer, 2006). The basic model is run for several simulations with different values of K and d70, which are in the range of (Sellmeijer, 2011). The model results of those simulations are compared with the results form the mathematical solutions of (Sellmeijer, 2011). The critical head difference are determined with the D-Geo Flow model and the method of Sellmeijer. As already described in Chapter 2.3, the critical head difference is the most important criterium in the assessment of piping.

Sellmeijer's solutions is based on a theoretical calculation model for backward erosion. The critical gradient is calculated, with equilibrium and the grains in the pipe just not moving, so the forces on the grain are in balance. If the actual gradient is smaller than the critical gradient, an equilibrium situation arises, in which the pipe no longer grows.

It is called failure when the channel grows beyond this equilibrium point. Because if the gradient is greater than the critical gradient, the pipe will develop completely into a continuous pipe. Eventually, this can cause the collapse and breach of the dike. (Vrijling, 2010) Currently, the Sellmeijer method is the official design standard for Levees in the Netherlands. Although this method is not valid for grain sizes larger than d70 which is 500 µm (Deltares, 2012). The critical gradient can be determined with the following set of equations:

$$\Delta H \leq \Delta H_c = L\, F_s\, F_R\, F_G \qquad \text{Equation 2}$$

$$F_s = \frac{d_{70}}{\sqrt[3]{kL}}\left(\frac{d_{70}}{d_{70m}}\right)^{0.4}$$ Equation 3

$$F_R = \eta\frac{\gamma_p'}{\gamma_w}\tan\theta$$ Equation 4

$$F_G = 0.91\left(\frac{D}{L}\right)^{\frac{0.28}{\left(\frac{D}{L}\right)^{2.8}-1}+0.04}$$ Equation 5

Where:

ΔH_c	The critical hydraulic gradient	(m)
L	The minimum seepage length	(m)
F_s	The scale factor	(-)
F_R	The resistance factor	(-)
F_G	The geometrical shape factor	(-)
d_{70}	The grain diameter for which 70 percent of particles are smaller	(m)
d_{70m}	The mean d70 in the small-scale tests (2.08·10−4)	(m)
K	The intrinsic permeability of the aquifer	(m^2)
η	White's constant	(-)
γ_p'	The unit weight of particles	(kN/m^3)
γ_w	The unit weight of water	(kN/m^3)
θ	The bedding angle	(°)
D	The thickness of the aquifer	(m)

The input parameters for equation 2, 3, 4 and 5 are given in Table 4. Those values are corresponding to the basic model.

Table 4. Input parameters of equation 2, 3, 4 and 5.

Parameter	Value
L	46.8
D70	0.0002
D70m	0.000208
$\boldsymbol{\eta}$	0.25
$\boldsymbol{\gamma_p'}$	2650
$\boldsymbol{\gamma_w}$	1000
$\boldsymbol{\theta}$	37
D	30

The simulations are done in stationary mode, since this corresponds with the configuration of the method of Sellmeijer because the results are independent from time. The results of this verification are shown in Table 5, where the difference between the D-GeoFlow model and the results proposed by the method of (Sellmeijer, 2011). The average difference between the D-GeoFlow model and the method is 1.06 %, therefore the model corresponds at a sufficient level with the method of Sellmeijer. Studies of (Van Rees, 2019) and (Stoop, 2018) had similar deviations in their verification; namely 1.32% and 5% respectively. Those studies also used a basic

D-Geo Flow model and compared the modelling results with the method of Sellmeijer. There can be several explanations for the deviation, for example, the grid definition of the model. When reducing the dimensions of a grid element, the model result would be more precise and deviation would be become <1.00%. But, reducing the dimensions of the grid would drastically increase the run time of the model.

Table 5. Verification results.

K [m/d]	D70 [µm]	Hc [m] model	Hc [m] Sellmeijer	Difference [m]	Difference [%]
5	200	4.77	4.83	0.05	1.05
10	200	3.79	3.83	0.04	1.06
2	200	6.45	6.55	0.10	1.55
3	300	6.63	6.73	0.08	1.21
5	100	3.63	3.66	0.03	0.83
10	200	3.78	3.83	0.05	1.32
20	150	2.70	2.71	0.01	0.37
			Average	0.05	1.06

3.2Schematization model

Now, the input parameters and boundaries of D-Geo Flow are verified with the method of Sellmeijer. As already mentioned, the verification model is not suitable during the experiments since it contains a homogenous aquifer. In this thesis, the gravel layer is located below a small sand layer, which also corresponds with information from the WBI Limburg. This is a cooperation between HKV, Witteveen+Bos, and, Waterschap Limburg. Therefore, the schematization model haves a small sand layer. In Figure 15, the difference between the aquifer-layer setup is shown.

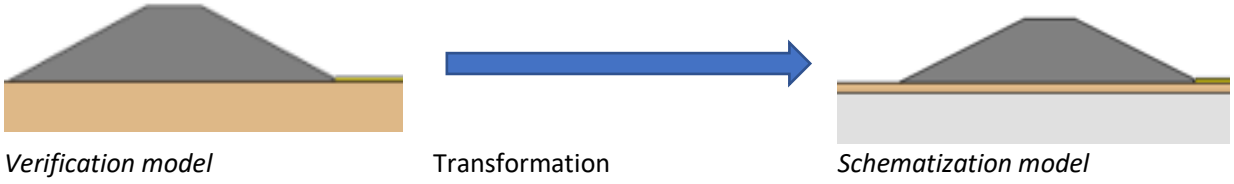

Figure 155. From the verification model to the schematization model.

This schematization model will be based on the verification model, since the settings of the verification model had only a deviation of 1.06% with the method of Sellmeijer. So, the model does correspond correctly to the method of Sellmeijer. The effect of the permeability of the gravel layer will be determined by increasing the permeability step-wise. In the other experiment, the thickness will be increased step-wise to determine the effect of the thickness on piping. The experiment will be more explained in Chapter 3.3 and 3.4.

3.2.1 The geometry

The schematization will be used adjusted during the experiments. The schematization model is the starting point of this study and is based on the settings of the verified model described in Chapter 3.1 and the geological properties of the layers are based on the information from the WBI Limburg. This schematization model can be found in Figure 16.

The geometry of the schematization model is equal to the geometry of the verification model. A small blanket of sand with low permeability is located below a relatively low levee and above a gravel layer with a large permeability. The gravel layer has a thickness of 10 meters and is located above an impermeable layer made

from limestone and marl, those are impermeable materials. The impermeable layer is represented by the no-flow boundary in the model. The dike has a seepage length of 46.8 meters. The height of the dike does not affect the groundwater flow since the compressibility of the materials is zero.

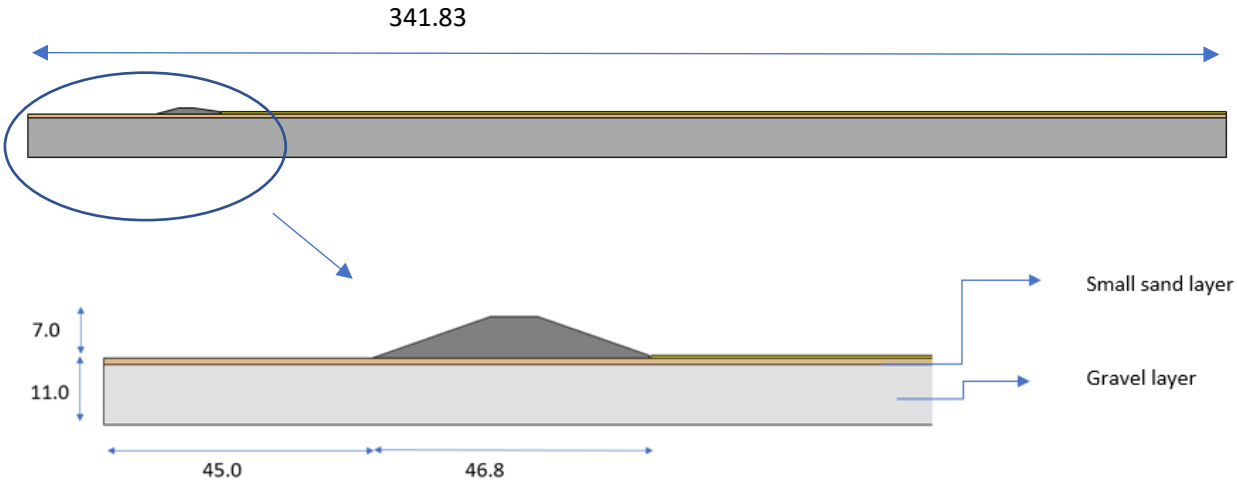

Figure 16. The geometry of the case. Dimensions in [m].

The geological properties of the different layers are given in Table 6. The particles in the gravel layer are not part of the piping mechanism therefore it is possible to use a d70 of 0.8 mm instead of 2.0 mm, which is the actual grain size. The D-Geoflow model consists of two parts: a groundwater flow model and the piping model. The gravel layer is only part of the groundwater flow model part in D-Geo Flow.

Table 6. Aquifer properties.

Layer	D70 (µm)	Permeability (m/d)
Clay	200	0.01
Sand	200	6.5
Gravel	800	250

3.2.2 Calculation options

Assessing with the D-GeoFlow is a relatively innovative way whereas another standard option is the determine the critical gradient according to the analytical equations of Sellmeijer. It is instructive to compare these two results which each other to see how big the deviation is between these options.

The design rule of Sellmeijer is validated for a homogenous subsurface whereas the schematization model has multiply different layers present in the subsurface. The variety of layers gives consequently multiply permeabilities and grain sizes. Therefore, a rule of thumb has been designed to assess these situations. The method of Sellmeijer gives only the option to implement the value of permeability. That is why the rule of thumb provides an effective permeability, which fits in the equation. The effective permeability is the result of the combined permeability of the stacked layers. The thickness-weighted arithmetic mean is commonly used when the upper layer is less permeable as the lower layer. The situation of the schematization model fits this condition and therefore the following equation is allowed:

$$k_{eff} = \frac{d_1 k_1 + d_2 k_2}{D}, \quad D = d_1 + d_2 \qquad \text{Equation 6}$$

The d_1 and k_1 represent the thickness and the permeability upper layer whereas the d_2 and k_2 belong to the thickness and the permeability of the lower layer. The values of the basic model are given in Table 6. The effective permeability of the subsurface in the model is 148.64 m/day. The value of d70, which will be used in the method of Sellmeijer, corresponds to the grains located directly below the impermeable layer of the dike since these grains are vulnerable to the piping mechanism. The d70 used for the assessment of the schematization model is given in Table 6.

Table 7. Input values to determine the effective permeability.

Layer	Thickness in [m]	Permeability in [m/day]	D70 in [µm]
1 (Sand)	1	6.5	200
2 (Gravel)	10	250	

It is interesting to see which method is more conservative to use during a piping assessment. Therefore, the critical head difference is calculated by the D-GeoFlow model and the adjusted design rule for multiply layers of Sellmeijer, this rule will be called from this point as 'Sellmeijer's formula'.

3.3Experiment 1: Effect of the permeability on piping

The schematization model introduced in Chapter 3.2 will be used as the standard model during the experiment. The effect of the permeability on the critical gradient will be determined in this experiment. This will be achieved by increasing the permeability of the gravel layer stepwise and keeping the other factors constant, so these do not impact the results of the experiment.

The permeability of the second layer will be increased stepwise from 6.5 until 400 m/day while all other materials, geometry and, boundary conditions stay constant in all steps. This experiment consists of 14 steps. Afterward, the effect of the permeability will be plotted against the critical gradient and the critical groundwater flow velocity to determine the effect of the permeability on the piping mechanism. The spreading's length used during this experiment are given in Appendix B. First, the groundwater flow velocity will be explained on the next page (23).

So, in each step will be the critical gradient and the water flow velocity in the pipe be calculated and afterward, these results will be plotted against permeability. This provides insight in the effect of the permeability of the gravel layer on the piping mechanism. Furthermore, the critical head difference calculated by the D-GeoFlow model will be compared with the proposed outcomes of the Sellmeijer's formula to determine which option gives a more conservative prediction.

3.4Experiment 2: Effect of the thickness on piping

Likewise, in the previous experiment, the schematization model will be used during the experiment. The effect of the permeability on the critical gradient will be determined in this experiment. This will be achieved by increasing the thickness of the gravel layer stepwise and measuring the critical gradient in each step. Also, the groundwater flow velocity in the pipe at the moment of failure will be measured in each step.

In each step will be thickness of the gravel layer in the schematization model adjusted. Secondly, the run is performed with that model. Afterward, the critical head difference will be noted and, the groundwater flow velocity in the pipe at the moment of failure will be measured in each step. The experiment will include in total of 8 simulations in which the thickness of the gravel layer will be increased from 1.00 meters until 75.00 meters. The spreading's length used during this experiment is given in Appendix B.

4 Results

This chapter contains the results of the schematization model and both performed experiments, consequently the last 2 research questions are answered; (iii) what is the effect of the thickness of the gravel layer on the piping mechanism?; (iv) what is the effect of the permeability of the gravel layer on the piping mechanism?.

4.1Result of the schematization model

The D-GeoFlow model based on the schematization provides in the 'Equilibrium Head Drop' output- option the possibility to display the gradient over the length of the pipe. This plot is given below in Figure 17. The critical head drop is the last head drop in the table before the pipe grows towards the other end of the dike. In the graph is the pipe length indicated on the x-axis. The pipe grows in the graph from the left-side (polder) to the right-side (river). The critical head difference for each part of the pipe is plotted, hence it is possible to select the critical head difference corresponding to the last part of the pipe before the pipe fully develops to the riverside. The indicated critical head difference in D-Geo Flow is the same as the critical gradient calculated with the design rules of Sellmeijer. Because, in this method is the critical gradient like the drop in which the pipe formation does not stop with constant load (Hart, 2018). The graph in Figure 17 is the applied head difference over the pipe length which corresponds to the schematization model.

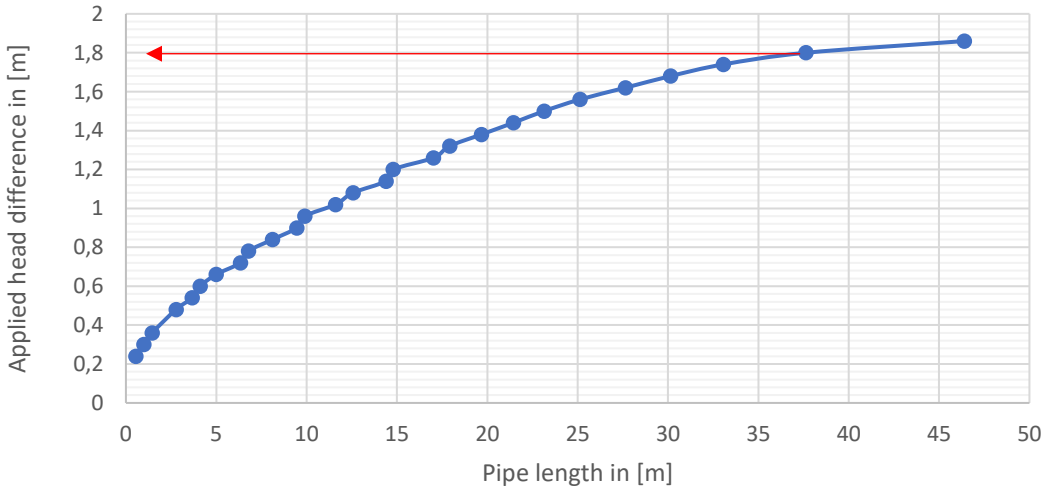

Figure 167. The applied head drop of the schematization model from D-Geo Flow (The red arrow indicates the critical head difference of the pipe).

The D-Geo Flow predicts a critical head difference of 1.80 meters and the Sellmeijer's formula forecasts a critical head difference of 2.10 meters. The difference between the two predictions is 30 centimetres, which is a difference of 16.67%, considering the D-Geo Flow prediction. The deviation is larger compared with the deviation of the verification model (1.06%) since the Sellmeijer's formula is a thumb rule and not validated for inhomogeneous layers. Therefore, the deviation between the two calculation options is much larger.

4.2Result of experiment 1: Effect of the permeability

This experiment was successfully performed in D-Geo Flow. The simulation output of the head difference and the flow velocity are worked out in Excel. The created plots are shown and explained in the following sections.

4.2.1 Critical head difference

Figure 18 is the result of increasing the permeability of the gravel layer and notes the critical head difference of each situation. From this graph can be concluded that the critical head difference decreases over the increase

of permeability. The curve has an asymptotic shape. The impact on the critical gradient is relatively large in situations where the permeability of the gravel layer is below 150 meters per day. The result of each single simulation run is given in Appendix C.

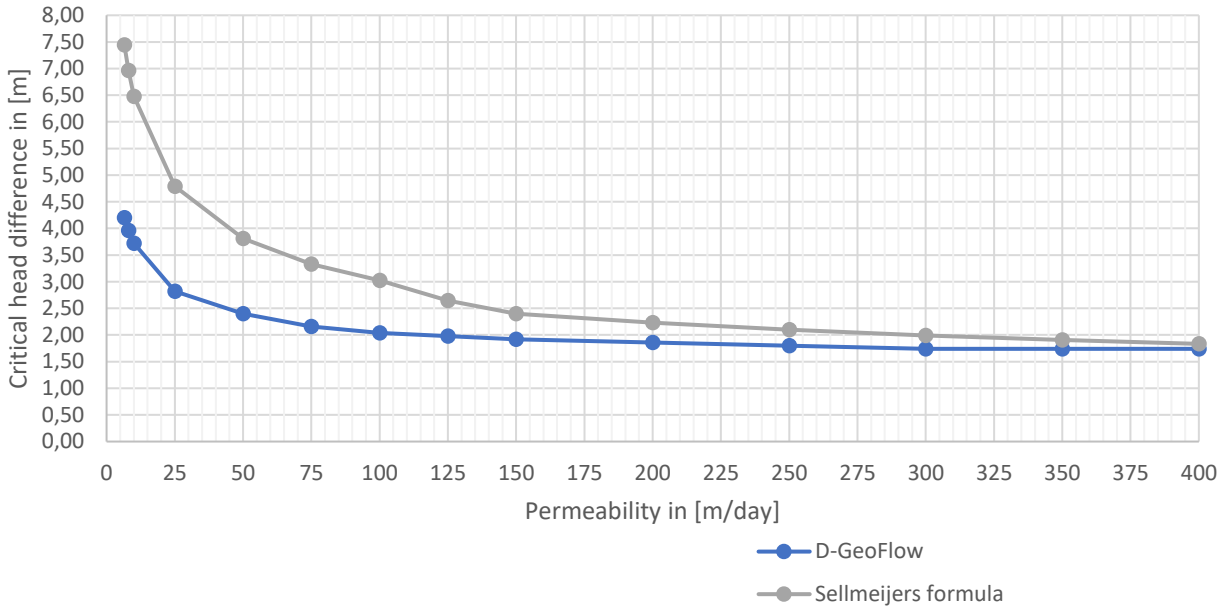

Figure 178. The permeability against the critical head difference.

Also, Table 8 shows that the impact on the critical head difference until 150 meters per day is relatively large in comparison with after 150 meters per day. When the permeability is larger than 300 meters per day, the critical head difference does not further decrease.

Table 8. Overview of the impact of the permeability. Calculated with D-Geo Flow.

Permeability in [m/day]	The corresponding critical head difference in [m]
6.5	4.20
150	1.92
Difference	***2.28***
150	1.92
400	1.74
Difference	***0.18***

In Figure 18 are also the proposed critical head differences according to the Sellmeijer's formula (earlier mentioned in Chapter 3.2) plotted in the graph. After observing the graph, there can be concluded that Sellmeijer's formula predicts a less conservative result for the critical head difference for every permeability of the gravel compared with the D-Geo Flow model. There can also be concluded that the deviation decreases over the increase of permeability. The deviation between the two methods becomes smaller when the permeability of the gravel layer increases. The field measurements of a gravel subsurface in Limburg gave permeabilities between 85 and 184 meters per day. (Koopmans & Janssen, 2018) The global profile of a dike in Limburg had a gravel layer with a permeability of 250 meters per day. This analysis has shown that the deviation

between the two calculation options is relatively large for the permeabilities between 85 and 184 meters per day. The deviation is smaller for permeabilities around the 250 meters per day, but still is the difference 30 centimetres which is equal to approximately 14%.

4.2.2 Critical flow velocity

The D-Geo Flow model can show the groundwater flow velocity in the pipe over the time-series. Thereby, the flow velocity at the critical head difference can be determined, which is the critical flow velocity. Figure 19 shows the velocity over the length of the pipe (offset) at a given moment in time. The right graph represents the velocity in the pipe just after the failure of the dike, whereas the left plot is the graph at the critical head difference. The highest velocity in the left figure is indicated with the red pointer. During the simulation of situations with different permeability will be this highest velocity measured and eventually plotted. In this case, the groundwater flows underneath the dike flows from the left to the right, where the river is located at the left-side and the polder at the right-side. Important for the interpretation of the result is to realize that the pipe grows from the left (polder) to the right (river). So, in the graphs shown in Figure 20 grows the pipe from the left (polder) to right (river).

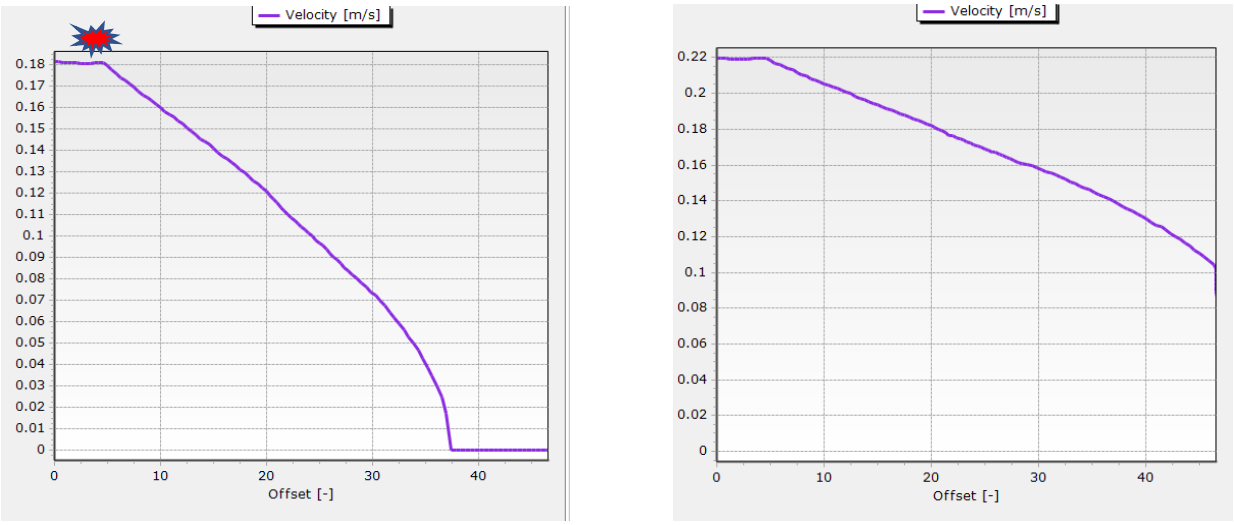

Figure 19. (left): the velocity in the pipe at the critical head difference. (right): the velocity in the pipe just after the pipe reaches the riverside.

A remarkable feature in the left graph of Figure 19 is that the velocity at the last part of the pipe is zero, whereas reality shows that there is a groundwater flow underneath the dike, which makes it impossible for the velocity to be zero. This feature can be simply explained by the structure of the model. In the graph grows the pipe from left (polder-side) to right (riverside). The pipe has not developed completely, because at the critical moment is the pipe not fully grown. The model does not record any flow velocity in the part of the pipe which is not developed yet. In short, this is due to the structure of the program. So, there is a groundwater flow through this part of the soil, but since it is not designated as pipe, the flow velocity is zero. Figure 20 shows the situation of the pipe at the critical moment. The blue boxes in the pipe are part of the pipe whereas the red boxes are not part of the pipe yet. So, in the red boxes is no flow velocity recorded can be seen in Figure 19 (left graph).

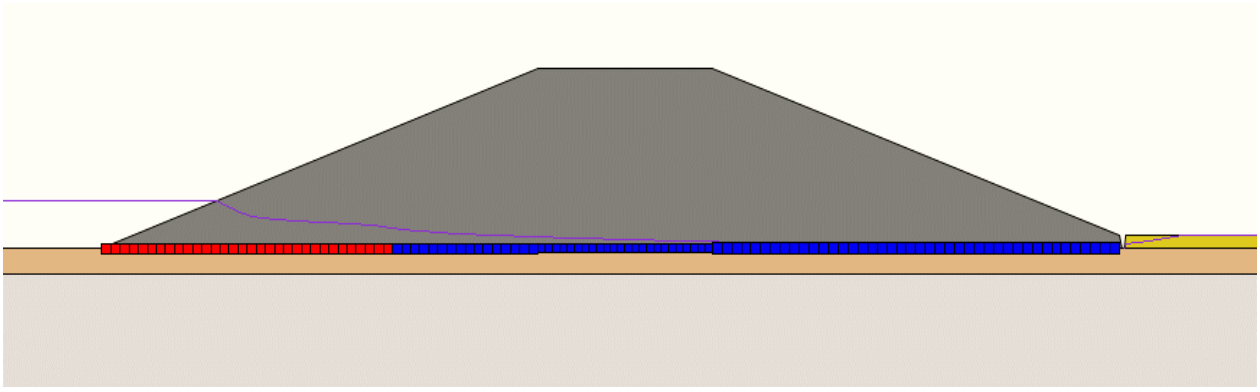

Figure 180. The situation in D-Geo Flow at the critical head difference. This is the last step before the pipe grows completed to the riverside.

The graph in Figure 21 contains the critical flow velocity in the pipe for different situations. In advance, there is expected that the critical velocity in the pipe would be constant over the increase in permeability. Since the geological properties of the sand layer do not change throughout the experiments, and therefore, the velocity required to move the particle would be the same. But, the results of the analysis have shown a different trend. Figure 21 shows the effect of the permeability on the velocity in the pipe. With the 'velocity in the pipe' is meant the groundwater velocity in the pipe at the moment when the pipe has reached its complete length. The trend-line through the points has a logarithmic shape because the water has a maximum flow velocity in the pipe due to gravity, etc.. According to these results, there is a higher velocity required to disturb the equilibrium and transport of the particles when the gravel layer is more permeable. A larger permeability gives more groundwater flow velocity in and around the pipe concerning to the difference between the open water level and the water level in the hinterland (head difference). Groundwater flow velocity increases faster with an increase in the permeability of the gravel. In short, piping occurs earlier (lower critical head difference) as a consequence of a higher groundwater flow velocity at a lower head difference due to the larger permeability in the gravel. To demonstrate with an example: gravel with a permeability of 150 m/d has a groundwater velocity of 1 at a head difference of 0.5 meters. Now, the permeability of the gravel is increased to 250 m/day. In this case, the velocity of 1 will be reached earlier at a lower head difference of 0.3. Due to the reason that the flow velocity is very decisive for the transport of particles, therefore the situation with 250 m/d in an earlier stage.

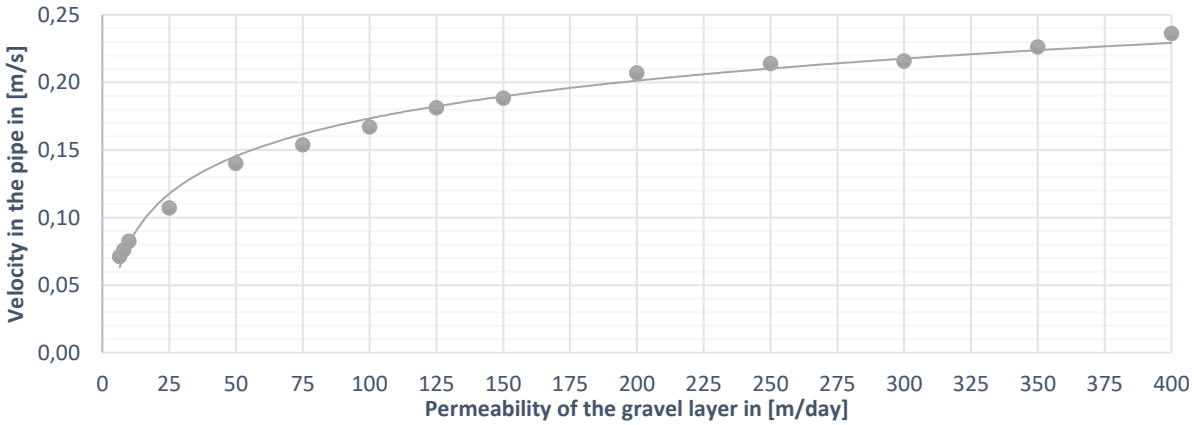

Figure 21. The effect of permeability on the critical flow velocity in the pipe.

4.2.3 Critical pipe-length

Another notable result in the analysis of the critical head difference is the place in the pipe where the critical head difference is exceeded. The point of failure in the pipe is located closer to the riverside when increasing the permeability of the gravel layer. This can be concluded after observing Figure 22 where the critical head difference over the length of the pipe is shown for different situations. The y-axis is varying between the graphs, but this does not relate to the critical length in the pipe. The pipe is growing from the polder-side to the riverside. So, the permeability does not only influence the critical head difference and critical velocity in the pipe but also on the point of failure in the pipe.

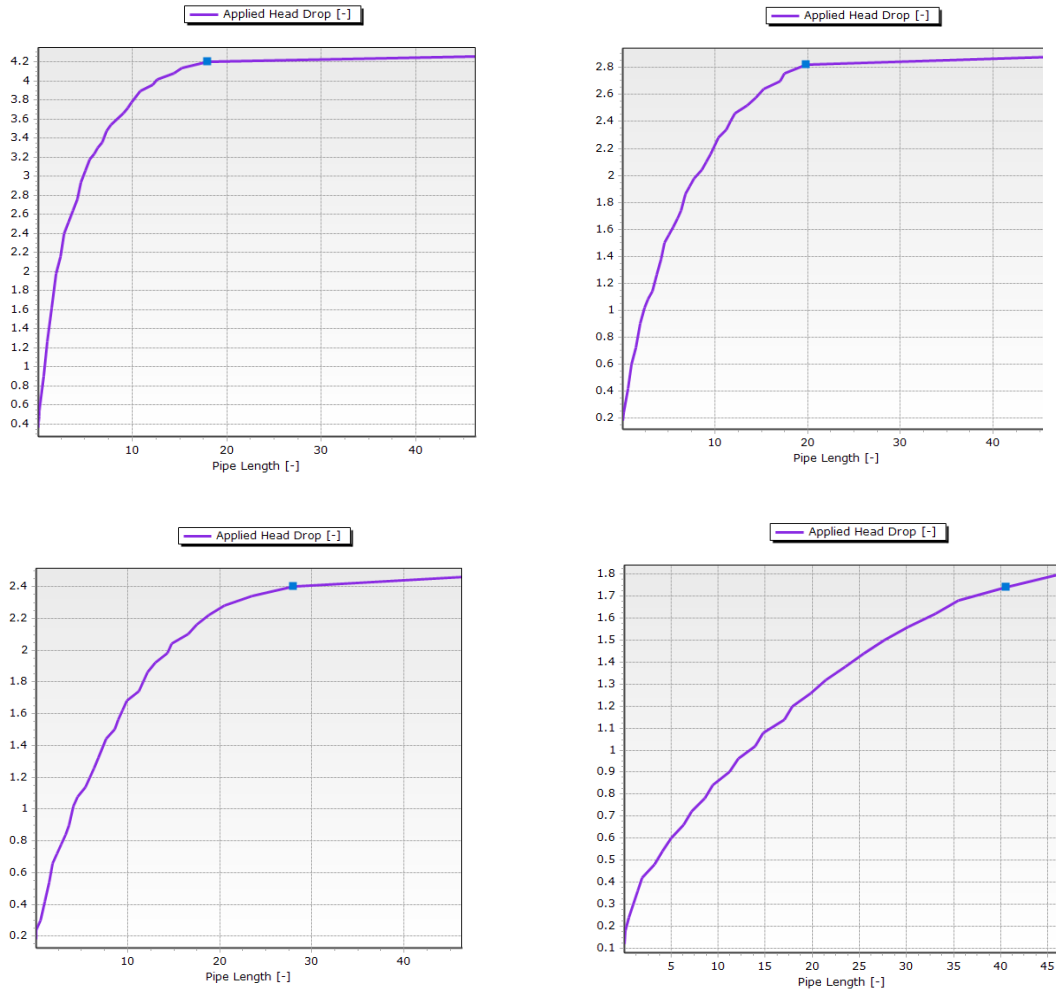

Figure 22. The changing critical pipe-length.

Table 9 provides information about the graphs shown in Figure 22.

Table 9. Graph information of Figure 22.

Graph	Permeability in [m/d]
Top left	6.5
Top right	25
Bottom left	50
Bottom right	400

The WBI uses the design rule of Sellmeijer with the critical point in the pipe was located at the middle of the seepage length (Roode, Maaskant, & Boon, 2019). The results of the D-GeoFlow experiment show that the critical point is not always located in the middle of the seepage length, but this point located in a wider range in the pipe.

4.3Result of experiment 2: Effect of the thickness

This experiment was successfully performed in D-Geo Flow. The simulation output of the head difference and the flow velocity are worked out in Excel. The created plots are shown and explained in the following sections.

4.3.1 Critical head difference

The results of this analysis are shown in Figure 23. From this graph can be confirmed that a thicker gravel layer leads to a lower critical head difference. To interpret the effect of a gravel layer on the critical head difference is the effect of the less permeable layer to see the effect of a gravel layer in perspective. The less permeable layer has a permeability of 60 meters per day.

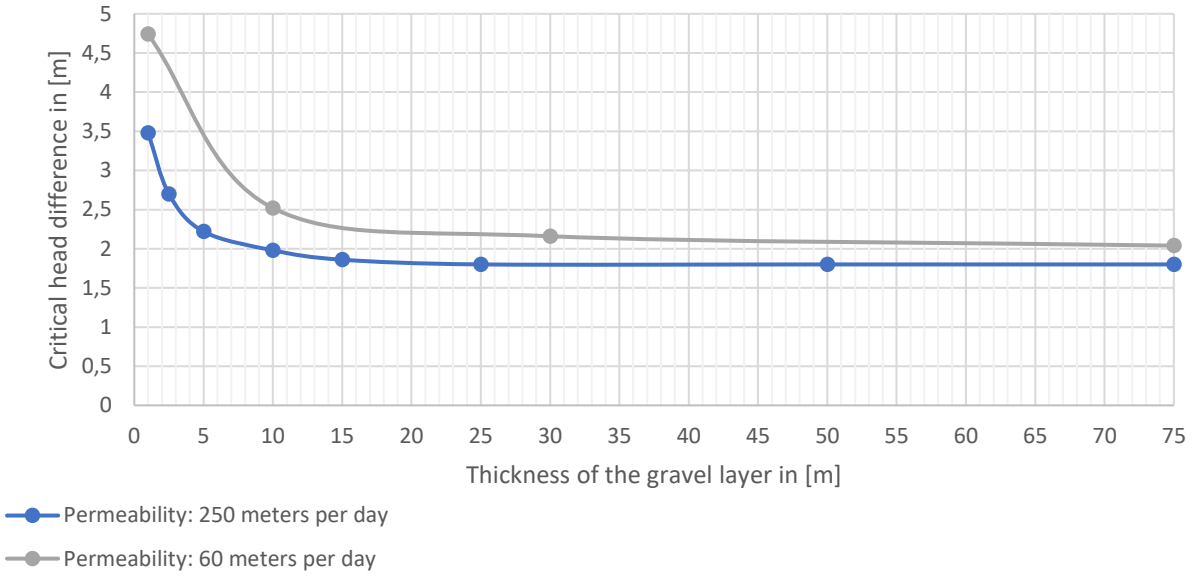

Figure 193. The effects of the thickness for a gravel layer and a less permeable layer.

The effect of thickness in the first 10 meters is relatively large. Also, it can be seen from the graph that the critical head difference with a thickness of 25 meters is equal to the critical head difference with a thickness of 70 meters. After a thickness of 25 meters is the effect of a thicker gravel layer negligible. Furthermore, from Figure 24 can be concluded that the Sellmeijer's formula was less conservative than the results of the D-GeoFlow models. The deviation between the two calculation options decreases over the increase of the thickness, although, the deviation stabilizes at a thickness of 45-50 meters. After observing the two curves in the graph, there can also be concluded that the curves have a similar shape.

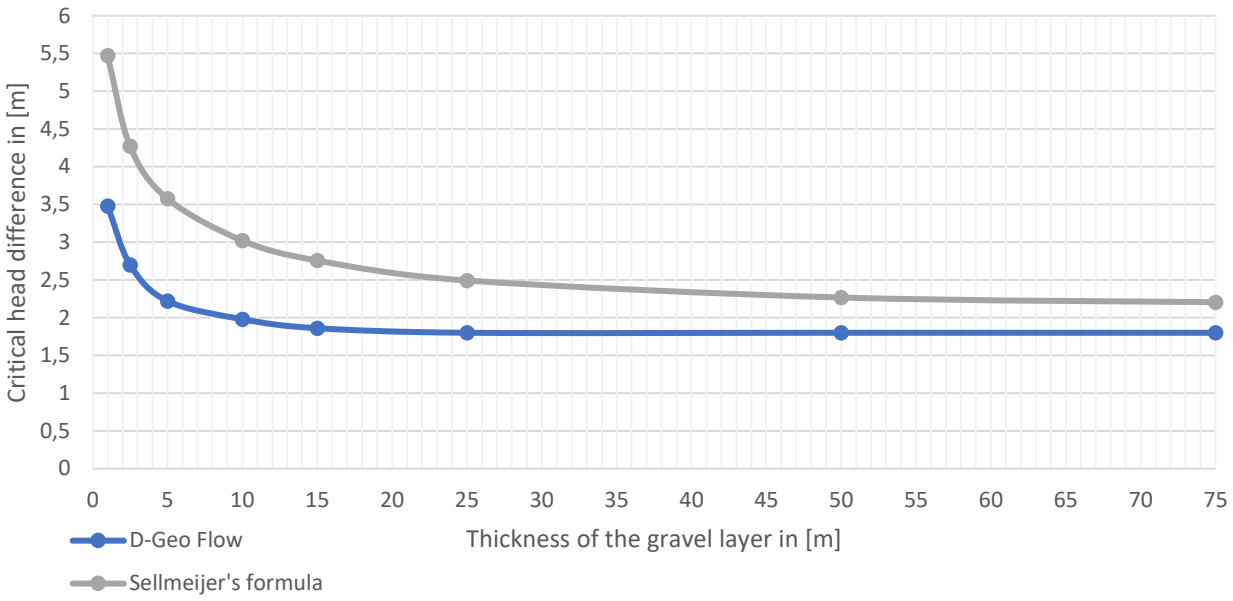

Figure 24. Effect of the thickness on the critical head difference

4.3.2 Critical flow velocity

The graph in Figure 25 shows the effect of the thickness of the gravel layer on the critical flow velocity in the pipe. This critical flow velocity is selected in the same way as in Chapter 4.2. There can also be concluded that the critical flow velocities do not further increase after a thickness of 50 meters and that the velocity increases rapidly in the first 25 meters.

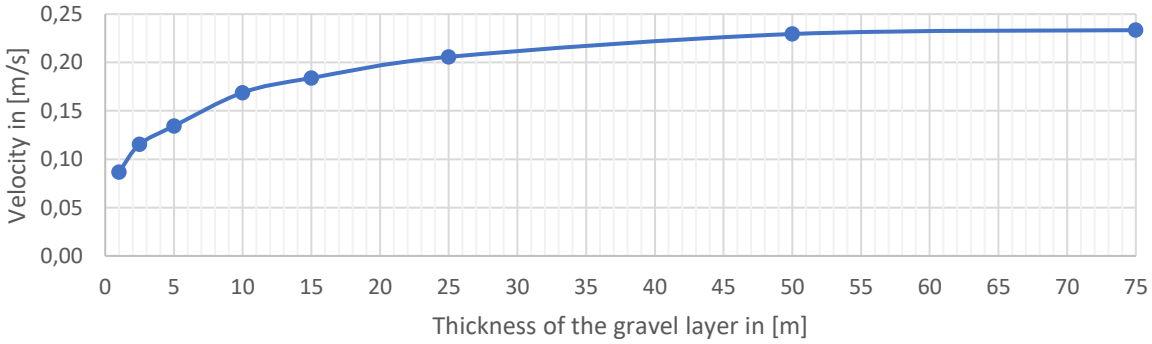

Figure 205. The effect of the thickness against the critical groundwater flow velocity in the pipe.

4.3.3 Critical pipe-length

The critical pipe-length behaves similar to the results in Chapter 4.2.3. The critical pipe-length increases when the critical head difference decreases.

5 Discussion

In this chapter will be critically reflect given on the results of this thesis. The limitations and remarkable results are discussed in the following points:

- Important to realize is that the results of this study are related to the specific settings used in D-Geo Flow modelling. The output result of D-Geo Flow can be more precise when using a more advanced grid or a boundary distance which is three times the spreading's length instead of two times. But, this would not directly impact the conclusions since the settings are the same in each simulation.
- Another remark, in D-Geo Flow, the pipe is considered to grow in the horizontal direction, whereas in reality, the pipe can grow in multiply directions due to the natural boundaries between the sand and clay layer (Wang, Chen, He, & He, 2016). What the effect of this limitation of the D-Geo Flow model is on the results is unknown, but it will probably impact the results.
- In addition, the pipe lengths were constant during all performed experiments, therefore this parameter cannot influence the results. But, the deviation between the critical head differences proposed by the Sellmeijer's formula and the D-Geo Flow model is not the same for all pipe lengths. The pipes used during the experiments had a length of 46.8 meters. The graph in Figure 26 shows the effect of the pipe length on the critical head difference for both calculation options. There can be concluded that experiments with a pipe length between 40 and 50 meters have the most possible deviation. This can explain the greatness of the deviation sometimes in the experiments. Although, from this graph can also be concluded that the Sellmeijer's formula is less conservative than the D-GeoFlow models for all pipe lengths in this research study. So, the conclusions about the conservatism of the two methods are still valid for this study.

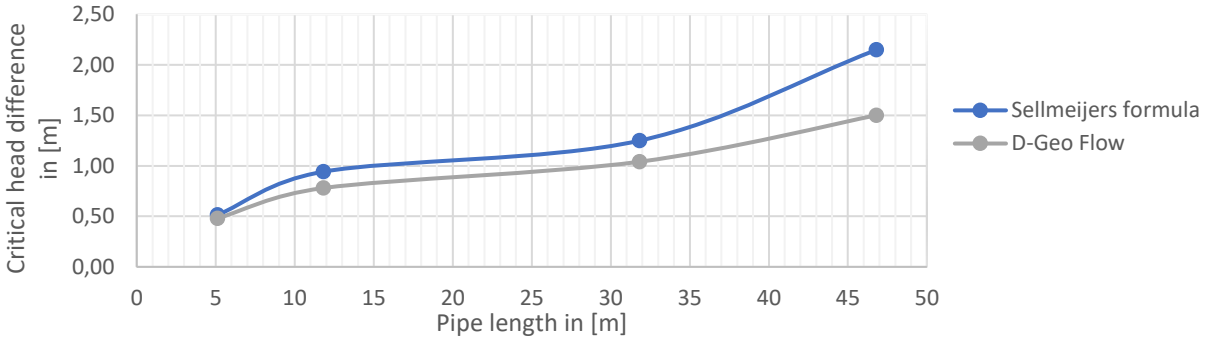

Figure 26. Effect of the pipe length on the deviation between the Sellmeijer's formula and D-Geo Flow.

- In the experiments, the pipe grew in the small sand layer with d70 of 200 µm and permeability of 6.5 meters per day. The study in Chapter 2.2 has shown that these two properties influence the piping mechanism, but during the experiments are these values kept constant. Therefore, these factors do not influence the actual results. But the results are strongly related to these parameters since other properties of the sand layer could influence the effect of the underlying gravel layer.
- There are many causes for the critical pipe length to shift. However, changing the input does not only change the pipe length but also the critical head difference. The critical pipe length, however, has no specific relationship to the critical head difference. More information is needed to provide a clearer answer (Deltares, 2020).
- One of the most remarkable results of this thesis is the variation in critical velocity over the critical head difference. A complete accepted clarification for this trend is not found in this thesis, although there is a presumption that the critical head difference is related to the critical velocity and vice versa.

The graph in Figure 27 confirms this presumption since the data from all performed simulations are located reasonably in one trend-line.

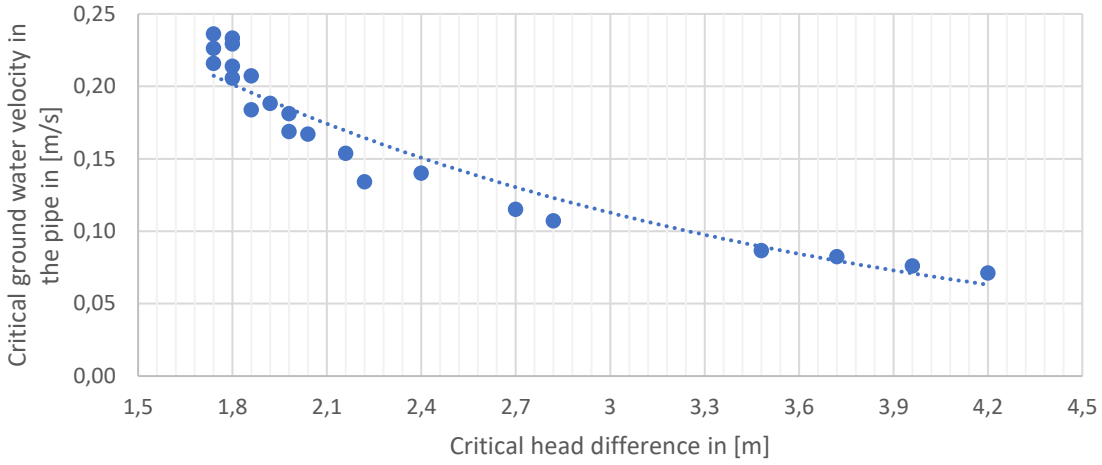

Figure 27. The critical groundwater velocity plotted against the corresponding critical head difference.

6 Conclusion

This chapter contains the summarized answers to the sub-question and the main question.

- *Sub-question 1: What are the hydrogeological effects of a gravel layer in the subsurface?*

Gravel layers have a relatively large permeability, which is largely depending on the percentage of sands covering the voids. This large permeability causes more groundwater flow in the soil, whereby higher flow velocities can be reached. Gravels have a larger volume thus also their weight is larger. Therefore, there is more pressure required to move the gravels and initiate the transport of particles. The sand particles are more vulnerable to move due to the groundwater flow when they are surrounded by gravels then by sands.

- *Sub-question 2: What factors influence the piping mechanism?*

The most important influencing factors on the piping mechanism are the following factors; thickness, permeability, grain size, seepage length and anisotropy. This thesis covers the factors which are relevant for gravel layers such as the permeability and the thickness. The grain size is also directly relevant for gravel layer, although the effect of this factors is not covered in this thesis since in D-Geo Flow was the pipe located in a sand layer

- *Sub-question 3: What are the effects of the permeability of the gravel layer on the piping mechanism?*

The analysis with D-Geo Flow and the Sellmeijer's formula has shown that a larger permeability decreases the critical head difference. The effect is negative exponential and has an asymptotic shape. In situations with permeabilities lower than 150 meters per day is the Sellmeijer's formula more conservative then the results of the D-Geo Flow models whereas situations in where the permeability of gravel layers are reached, the difference between the two analysis is negligible.

Furthermore, the analysis has shown that the critical groundwater flow velocities in the pipe are larger in situations with large gravel permeabilities then with lower permeabilities.

The critical pipe-length is depending on the critical head difference. A large permeability is causing relatively small critical head differences which is resulting in longer critical pipe-lengths and are located closer to the rivers-side of the dike.

- *Sub-question 4: What are the effects of the thickness of the gravel layer on the piping mechanism?*

The effect of thickness on piping is very similar to the effects of the permeability. They are both related to the groundwater flow in the system. Large permeabilities are causing large water flows nearby the pipe whereas the thickness attracts also more groundwater flows. The analysis with D-Geo Flow and the Sellmeijer's formula

has shown that a larger thickness decreases the critical head difference. The effect of the permeability decreases exponentially and has an asymptotic shape.
Gravel layers with a thickness larger than 15 meters do not influence the critical head difference more since the effect has an exponential asymptotic shape.
Since the critical pipe-length is depending on the critical head difference, the thickness also effects the critical pipe-length in the same way as the permeability did.

Main conclusion
This thesis has shown that a gravel layer in the subsurface has three significant effects on the piping mechanism.

1. **Decreases the critical head difference.** The gravel layer below the sand layer decreases the critical head difference. The number of decrease is depending on the permeability and the thickness of the gravel layer. Because when the gravel layer is very permeable or thick, the critical head difference becomes lower.
2. **Decrease in critical groundwater flow velocity in the pipe.** In situations where a gravel layer is in the subsurface, there is more ground water velocity in the pipe required to fully develop the pipe to the other side of the dike. There is expected that the decrease in critical head difference cause higher critical groundwater flow velocities in the pipe.
3. **Changing critical pipe-length.** The gravel layer impacts the critical pipe-length. There can be concluded that the critical pipe-length of a gravel layer is located closer to the riverside of the dike then in situations with a less permeable layer. So, the critical pipe-length is changing due to the gravel layer underneath the dike.

7 Recommendations

From this thesis study can be recommended to perform D-Geo Flow analysis in situations with multiply layers in the subsurface. Since the results of the D-Geo Flow models have shown to be less conservative than the outcomes of the Sellmeijer's formula. In other words, to ensure a safe situation, the D-Geo Flow needs to be used because it predicts lower critical head difference, which will appear more than the higher predicted critical head difference of the Sellmeijer's formula.
To broadly apply the insights regarding the effects of gravel layers from this thesis, the following subjects should be further investigated.

1. Model validation
   It is recommended to perform laboratory or field experiments to validate the results of this thesis. Since this thesis study is entirely performed in the program D-Geo Flow. Although, it will be very complex to measure the critical groundwater velocity in the field experiments. The validation can lead eventually to selecting the best calculation option. At this moment is it not possible to determine which calculation option is better.
2. Further research
   More research is required to declare the increase of critical groundwater flow velocity when the critical head differences decrease. This effect is not in line with expectations. The flow velocity is depending on many different factors in the model, whereby more research is needed to clarify this effect.
3. D-Geo Flow
   The program is recently developed and is not officially released at this moment. This study has used the D-Geo Flow version 1.0.3957. There must be noticed that this version is very time-consuming to do complex analysis. Therefore, it is recommended to further improve the usability of the program.

8 References

De Glee, G. (1930). *Over grondwaterstroomingen bij waterontrekking door middel van putten.* Delft, The Netherlands: Proefschrift Technische Hoogeschool Delft. . Retrieved from grondwaterformules.nl: http://www.grondwaterformules.nl/index.php/formules/onttrekking/deklaag-zonder-rand-de-glee

Deltares. (2012). *Onderzoeksrapport zandmeevoerende wellen (1202123-003-GEO-0002).* Rijkswaterstaat Waterdienst.

Deltares. (2020). *D-Geo Flow*. Retrieved from Deltares.nl: https://www.deltares.nl/nl/software/d-geo-flow/

Dutchwatersector. (2013). *Dutch and German dike experts held post flood field investigation along Elbe river, Germany*. Retrieved from Dutchwatersector: https://www.dutchwatersector.com/news/dutch-and-german-dike-experts-held-post-flood-field-investigation-along-elbe-river-germany

Fryar, A., & Mukherjee, A. (2019). *Groundwater Hydrology.* Reference Module in Earth Systems and Environmental Sciences.

Gupta, P., Alam, J., & Muzzammil, M. (2016). *Influence of thickness and position of the individual layer on the permeability of the stratified soil.* Aligarh, India: Civil Engineering Department, Aligarh Muslim University.

Hart, R. (2018). *Fenomenologische beschrijving.* Deltares.

Hoffmans, G., & Van Rijn, L. (2017). Hydraulic approach for predicting piping in dikes. *Journal of Hydraulic Research*.

Koopmans, R., & Janssen, W. (2018). *POV Piping - Invloed maasklei en grindlagen.* Arcadis.

Mulqueen, J. (2005). *The flow of water through gravels.* Teagasc, c/o Department of Civil Engineering, National University of Ireland, Galway.

Rijkswaterstaat. (2020). *Onttrekken grondwater, schematisatie van de voeding voor grondwatermodellering.* Retrieved from Richtlijn herstel en beheer (water)bodemkwaliteit: https://www.bodemrichtlijn.nl/Bibliotheek/bodemsaneringstechnieken/b-in-situ-reiniging/b4-fysische-technieken/b4-1-spoelen-met-grondwater/onttrekken-grondwater-schematisatie-van-de-voeding-voor-grondwate8589

Roode, N., Maaskant, B., & Boon, M. (2019). *Handreiking Voorland.* Projectoverstijgende Verkenning Voorlanden.

Sellmeijer J.B., L. d. (2011). *Fine-tuning of the piping model through small-scale, medium-scale and IJkdijk experiments.* European Journal of Environmental and Civil Engineering 15(8): 1139-1154. .

Sellmeijer, J. (2006). *Numerical computation of seepage erosion below dams (piping).* . Gouda, The Netherlands. : Proceedings Third International Conference on Scour and Erosion, 596-601, CURNET, .

Skempton, B. (1994). Experiments on piping in sandy gravels. *Geotechnique*, 449-460.

Standardization, I. O. (2002). *Geotechnical investigation and testing – Identification and classification of soil – Part 1: Identification and description".* International Organization for Standardization (ISO).

Stoop, N. (2018). *The effects of anisotropy and heterogeneity in the piping sensitive layer.* Delft: TU Delft.

Terzaghi, K. (1925). *Erdbaumechanik.* Vienna: Deuticke.

Texas Geosciences. (2020). *Some Useful Numbers on the Engineering Properties of Materials (Geologic and Otherwise).* Retrieved from The university of Texas at Austin Jackson School of Geoscience: https://www.jsg.utexas.edu/tyzhu/files/Some-Useful-Numbers.pdf

Tikkanen, A. (2020). *Earth Sciences.* Retrieved from Encyclopaedia Britannica: https://www.britannica.com/science/gravel

UC Denver. (2020). *Porosity and Permeability*. Retrieved from deq.louisiana.gov: https://www.deq.louisiana.gov/assets/docs/Water/DWPP_forkidsandeducators/PorosityandPermeability.pdf

Van Beek, V.M. (2018). *Pipinggevoeligheid grind en grindhoudende zanden Maasvallei.* Deltares.

Van Beek, V.M. (2015). *Backward erosion piping. Initiation and progression.*

Van Beek, V.M., & Robbins, B. (2015). Backward erosion piping: A historical review and discussion of influential factors". *ASDSO Dam Safety*.

Van der Gaast, J., & Massop, T. (2003). *Spreidingslengte voor het beheersgebied van Waterschap Veluwe.* Wageningen: Altera, Research Instituut voor de Groene Ruimte.

Van Rees, R. (2019). *Het modelleren van het buitendijkse grondwatersysteem.* Wageningen: Wageningen university and reserach.

Vrijling, J. K. (2010). *Piping -Realiteit of Rekenfout?Technical report, Dutch Expertise Network on Flood Protection (ENW).*

Wang, Chen, He, & He. (2016). *Experimental study on piping in sandy gravel foundations considering effect of overlying clay.* Water Science and Engineering.

Wiersma, A., & Hijma, M. (2018). *Korrelgroottes en heterogeniteit van rivierafzettingen in het licht van piping.* Deltares.

Appendix

Appendix A

D-Geo Flow model

The program D-Geo Flow is developed by Deltares in collaboration with Rijkswaterstaat. D-Geo Flow is a beta program which is still under construction by Deltares. The program is not officially released, although it used as support tool in recent projects of Witteveen + Bos. D-Geo Flow has been successfully applied in some test cases. (Deltares, 2020) The D-Geo Flow version 1.0.39057 is used during this thesis. The program can assess if piping occurs at a given head difference.

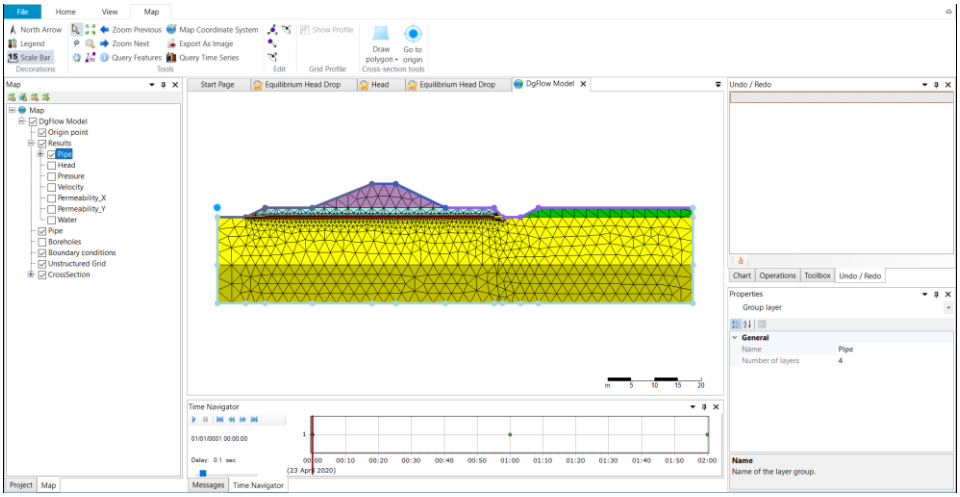

Figure 21. User-interface of D-Geo Flow

The piping mechanism in the program is based on the design rules of Sellmeijer. In D-Geo Flow, it is possible to perform 2D transient and stationary groundwater flow calculations with layered soil structure, in which a time-dependent hydraulic load, the compressibility of the grain skeleton and the groundwater, and change of the phreatic line are included. The program models the development of the pipe based on the flow in the pipe and the equilibrium of the grains combined with a groundwater flow simulator (Noordam, 2017). The option to implement multi-layer dike situations makes this program suitable for this thesis project.

The implemented pipe in the model is divided into small boxes by the grid function. The program calculates the equilibrium of the boxes. In each time-step, this equilibrium assessment is performed. When the equilibrium of the box is gone, the pipe will involve in that box. In each time-step will the program assess all boxes in the pipe. The critical gradient of the dike is reached, the pipe is fully developed, and the stability of the dike has failed.

Appendix B

Boundary distance

The distances of the left and right vertical boundaries have a significant effect on the outcome of the results. The distance the left vertical boundary and the dike has been determined by the local situation such as the foreland. The distance of the right vertical boundary in the model needs to be calculated with the spreading's length. The spreading's length is a measure of length (in meters) for the distance over which the groundwater reduction due to extraction will be noticeable (Van der Gaast & Massop, 2003).

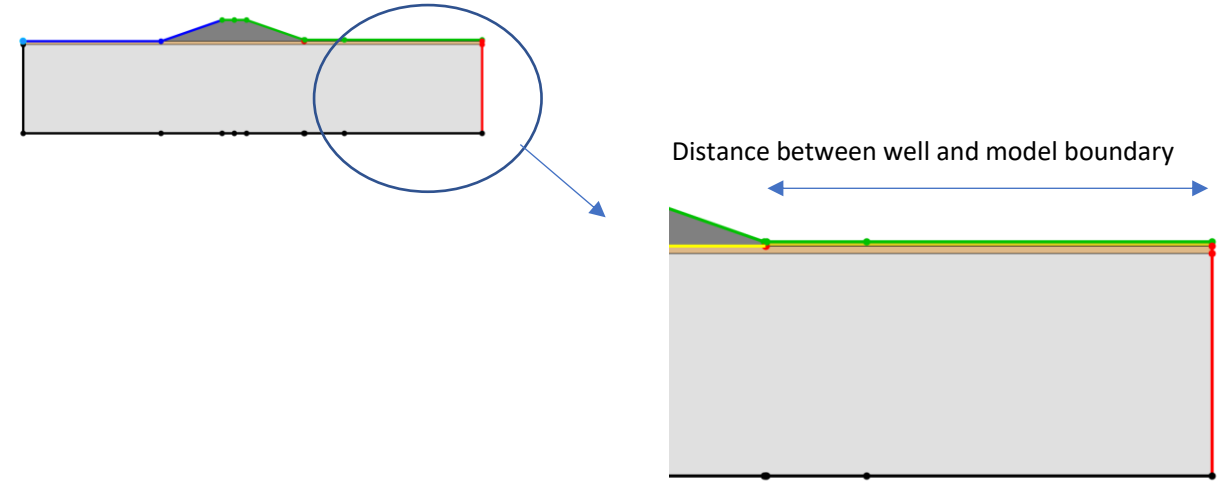

Figure . The boundary distance in the model.

The impact of the vertical right boundary should be limited; therefore, this model boundary should be placed at such a place the impact is negligible. The ditch represents the well in the model. This well is extracting groundwater from the aquifer. The extraction of the well has its effect on the groundwater table in the surrounding area of the well. The result is a groundwater table like the one in Figure 11. The blue curve in the figure is the water table. From the figure can be concluded that the effect of the water extraction is negligible at a certain distance, the spreading's length.

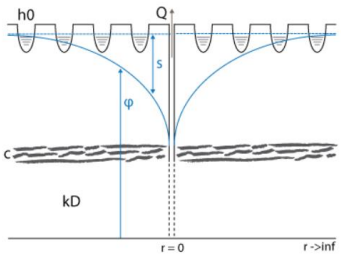

Figure . The impact on the ground water table from the water extraction of the well. **(De Glee, 1930)**

The spreading's length can be determined according the following formula (Van der Gaast & Massop, 2003):

$$\lambda = \sqrt{kDc}$$

Where:

K *The permeability in meters per day.*

D *The thickness of the aquifer in meters.*

c *The resistance of the covering layer in days.*

This effective permeability will also be used to determine the spreading's length, since the subsurface consist out of multiply layers. In short, the effective permeability is the average permeability of the combined layers, but this will be explained in the next section. The selected c-value can be calculated with the following formula:

$$c = \frac{d}{K}$$

The c-value can be calculated with the data given in Table 9. The calculated c-value is 25 days, which will be used to calculated the spreading's length.

Table 10. Parameters corresponding to the covering layer and the calculated c-value.

Parameter	Value
d	0.5 m
K	0.02 m/d
C	25 d

The spreading's length can be calculated with the data given in Table 10. This calculation will give a spreading's length of 86.10 meters. The model boundary should be so far away from the intervention that the rise in height at the model boundary by that intervention is negligible. Therefore, the model boundary should be at least at distance of 3 times the spreading's length. (De Glee, 1930) Thus, the boundary distance is 258.3 meters.

Table 11. Input parameters for the spreading length equation and the corresponding spreading length.

Parameter	Value
K	
D	10 m
C	25 d
λ	86.10 m

Spreading's length used during the experiment 'effect of the thicknesses.

The spreading's length is already introduced in Chapter 3.1 and depending on thickness of the aquifer; therefore, the boundary distance needs to be adjusted in each simulation to ensure that the thickness is the only parameter which affects the outcomes. The spreading length is calculated according the formula explained in Chapter 3.1. The table below gives the spreading's lengths used during the simulations.

Thickness of the gravel layer in [m]	Spreading's length in [m]
1.00	80.08
2.50	125.65
5.00	177.24
10.00	250.32
15.00	306.45
25.00	395.49
50.00	559.16
75.00	684.77

The boundary distance has a significant effect on the run-time of the model, therefore is chosen to use a boundary distance of two times the spreading's length. To give an indication, a boundary distance of 500 meters corresponds already to a run-time over 25 minutes whereas a model with a boundary distance of 50 meters runs in less than 3 minutes.

Spreading's length used during the experiment 'effect of the permeability'.

The spreading's length is also influenced by the permeability of the aquifer; therefore, the spreading lengths also vary in the simulations corresponding to this experiment. The table below provides the spreading lengths used in this experiment.

Permeability in [m/day]	Spreading's length in [m]
6.5	69.82
8	77.22
10	86.10
25	135.23
50	190.82
75	233.53
100	269.56
125	330.02
150	381.00
200	425.93
250	466.54
300	503.90
350	538.67
400	571.33

Appendix C

This D-Geo Flow output from the permeability experiment.

Permeability: 6.5 m/d

Pipe Length [-]	Applied Head Drop [-]
0.99048	1.26
1.4357	1.62
1.881	1.98
2.3262	2.16
2.7714	2.4
3.2167	2.52
3.6619	2.64
4.1071	2.76
4.5524	2.94
4.9976	3.06
5.4429	3.18
5.8881	3.24
6.3333	3.3
6.7786	3.36
7.2238	3.48
7.669	3.54
9.0048	3.66
9.45	3.72
9.8952	3.78
10.786	3.9
12.121	3.96
12.567	4.02
14.348	4.08
15.238	4.14
17.91	4.2
46.383	4.26

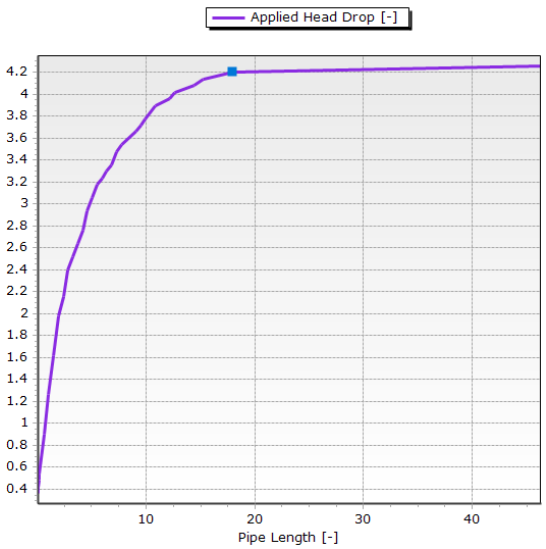

Permeability: 10 m/d

Pipe Length [-]	Applied Head Drop [-]
2.3262	1.68
2.7714	1.86
3.2167	1.98
3.6619	2.1
4.1071	2.22
4.5524	2.4
4.9976	2.46
5.4429	2.58
5.8881	2.64
6.3333	2.7
6.7786	2.82
7.2238	2.88
7.669	3
8.5595	3.06
9.0048	3.12
9.45	3.18
9.8952	3.24
10.34	3.3
11.676	3.36
12.121	3.42
12.567	3.48
14.348	3.54
15.238	3.6
17.464	3.66
19.8	3.72
46.383	3.78

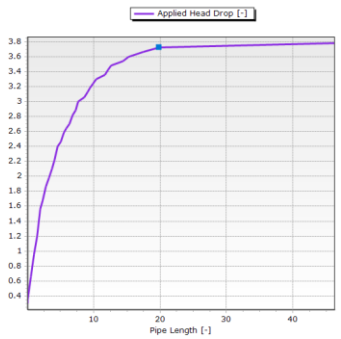

Permeability: 25 m/d

Pipe Length [-]	Applied Head Drop [-]
2.7714	1.08
3.2167	1.14
3.6619	1.26
4.1071	1.38
4.5524	1.5
4.9976	1.56
5.4429	1.62
5.8881	1.68
6.3333	1.74
6.7786	1.86
7.2238	1.92
7.669	1.98
8.5595	2.04
9.0048	2.1
9.45	2.16
10.34	2.28
11.231	2.34
11.676	2.4
12.121	2.46
13.457	2.52
14.348	2.58
15.238	2.64
17.019	2.7
17.464	2.76
19.8	2.82
46.383	2.88

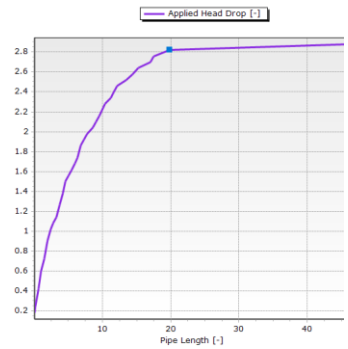

Permeability: 50 m/d

Pipe Length [-]	Applied Head Drop [-]
3.2167	0.84
3.6619	0.9
4.1071	1.02
4.5524	1.08
5.4429	1.14
5.8881	1.2
6.3333	1.26
6.7786	1.32
7.669	1.44
8.5595	1.5
9.0048	1.56
9.45	1.62
9.8952	1.68
11.231	1.74
11.676	1.8
12.121	1.86
13.012	1.92
14.348	1.98
14.793	2.04
16.574	2.1
17.464	2.16
18.8	2.22
20.467	2.28
23.467	2.34
28.05	2.4
46.383	2.46

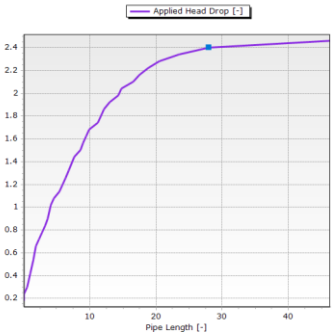

Permeability: 75 m/d

Pipe Length [-]	Applied Head Drop [-]
3.2167	0.72
3.6619	0.78
4.1071	0.84
4.5524	0.9
5.4429	0.96
5.8881	1.02
6.3333	1.08
6.7786	1.14
7.669	1.2
8.5595	1.26
9.0048	1.32
9.45	1.38
10.34	1.44
11.231	1.5
12.121	1.56
12.567	1.62
13.902	1.68
14.793	1.74
15.683	1.8
17.019	1.86
17.91	1.92
19.8	1.98
21.467	2.04
23.8	2.1
28.05	2.16
46.383	2.22

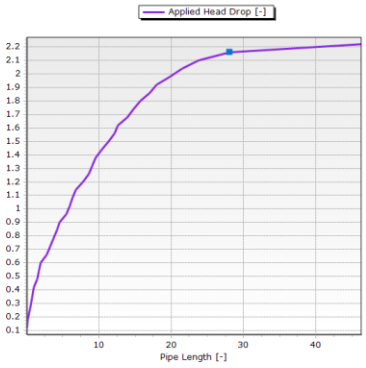

Permeability: 100 m/d

Pipe Length [-]	Applied Head Drop [-]
2.7714	0.6
3.2167	0.66
3.6619	0.72
4.1071	0.78
4.9976	0.84
5.8881	0.9
6.3333	0.96
6.7786	1.02
7.669	1.08
8.5595	1.14
9.45	1.2
9.8952	1.26
11.231	1.32
11.676	1.38
12.567	1.44
13.902	1.5
14.793	1.56
15.683	1.62
17.019	1.68
17.91	1.74
19.8	1.8
21.467	1.86
23.467	1.92
25.8	1.98
30.133	2.04
46.383	2.1

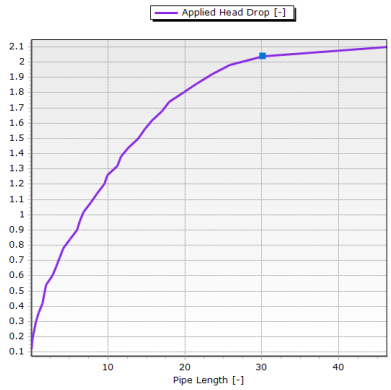

Permeability: 150 m/d

Pipe Length [-]	Applied Head Drop [-]
1.881	0.48
2.7714	0.54
3.6619	0.6
4.1071	0.66
4.5524	0.72
5.8881	0.78
6.3333	0.84
6.7786	0.9
8.1143	0.96
9.0048	1.02
9.45	1.08
10.786	1.14
11.676	1.2
12.567	1.26
13.902	1.32
14.793	1.38
16.574	1.44
17.464	1.5
19.133	1.56
20.133	1.62
22.133	1.68
23.8	1.74
26.133	1.8
30.133	1.86
33.467	1.92
46.383	1.98

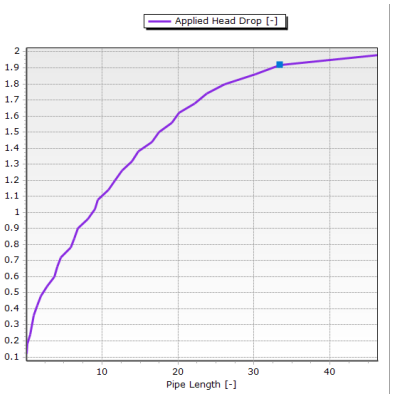

Permeability: 200 m/d

Pipe Length [-]	Applied Head Drop [-]
1.4357	0.36
2.3262	0.48
3.2167	0.54
3.6619	0.6
4.5524	0.66
5.8881	0.72
6.3333	0.78
7.2238	0.84
8.5595	0.9
9.45	0.96
9.8952	1.02
11.676	1.08
12.121	1.14
13.902	1.2
14.793	1.26
16.574	1.32
17.464	1.38
19.133	1.44
20.467	1.5
22.133	1.56
23.8	1.62
26.133	1.68
28.467	1.74
32.633	1.8
38.05	1.86
46.383	1.92

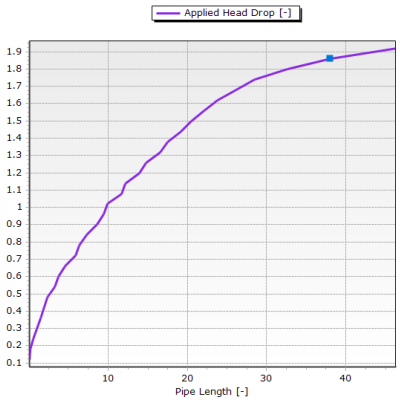

Permeability: 250 m/d

Pipe Length [-]	Applied Head Drop [-]
0.54524	0.24
0.99048	0.3
1.4357	0.36
2.7714	0.48
3.6619	0.54
4.1071	0.6
4.9976	0.66
6.3333	0.72
6.7786	0.78
8.1143	0.84
9.45	0.9
9.8952	0.96
11.676	1.02
12.567	1.08
14.348	1.14
14.793	1.2
17.019	1.26
17.91	1.32
19.467	1.38
21.467	1.44
23.133	1.5
25.133	1.56
27.633	1.62
30.133	1.68
33.05	1.74
37.633	1.8
46.383	1.86

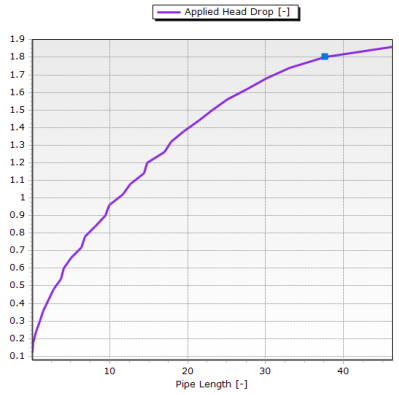

Permeability: 300 m/d

Pipe Length [-]	Applied Head Drop [-]
0.99048	0.3
1.4357	0.36
1.881	0.42
2.7714	0.48
3.6619	0.54
4.5524	0.6
5.8881	0.66
6.7786	0.72
7.2238	0.78
9.0048	0.84
9.45	0.9
11.231	0.96
12.121	1.02
13.902	1.08
14.793	1.14
16.574	1.2
17.464	1.26
19.467	1.32
21.467	1.38
23.133	1.44
25.133	1.5
27.217	1.56
29.717	1.62
32.633	1.68
35.55	1.74
46.383	1.8

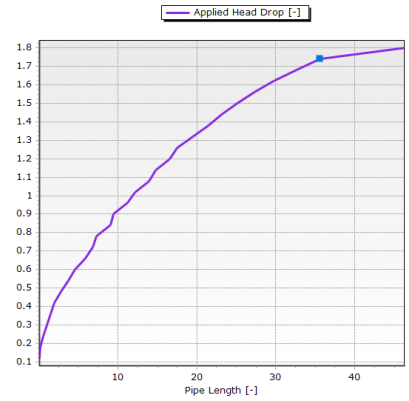

Permeability: 400 m/d

Pipe Length [-]	Applied Head Drop [-]
0.99048	0.3
1.4357	0.36
1.881	0.42
3.2167	0.48
4.1071	0.54
4.9976	0.6
6.3333	0.66
7.2238	0.72
8.5595	0.78
9.45	0.84
11.231	0.9
12.121	0.96
13.902	1.02
14.793	1.08
17.019	1.14
17.91	1.2
19.8	1.26
21.467	1.32
23.467	1.38
25.467	1.44
27.633	1.5
30.133	1.56
33.05	1.62
35.55	1.68
40.55	1.74
46.383	1.8